Comprehensive review on surfactant adsorption on mineral surfaces in chemical enhanced oil recovery

Liu, Zilong; Zhao, Ge; Brewer, Mark; Lv, Qichao; Sudhölter, Ernst J.R.

DOI
10.1016/j.cis.2021.102467

Publication date
2021

Document Version
Accepted author manuscript

Published in
Advances in Colloid and Interface Science

Comprehensive Review on Surfactant Adsorption on Mineral Surfaces in Chemical Enhanced Oil Recovery

Zilong Liu[*,†,‡], Ge Zhao[†], Mark Brewer[§], Qichao Lv[*,†], and Ernst J. R. Sudhölter[*,‡]

[†]Beijing Key Laboratory of Optical Detection Technology for Oil and Gas, College of Science, Unconventional Petroleum Research Institute, China University of Petroleum (Beijing), Beijing 102249, PR China

[‡]Organic Materials & Interfaces, Department of Chemical Engineering, Faculty of Applied Sciences, Delft University of Technology, Van der Maasweg 9, 2629 HZ Delft, The Netherlands

[§]Shell Global Solutions International B.V., Shell Technology Centre Amsterdam (STCA), Grasweg 31, 1031 HW, Amsterdam, The Netherlands

Corresponding authors

E-mail: zlliu89@gmail.com (Z.L.).

E-mail: lvqc@cup.edu.cn (Q.L.).

E-mail: E.J.R.Sudholter@tudelft.nl (E.J.R.S.).

Abstract

With the increasing demand for efficient extraction of residual oil, enhanced oil recovery (EOR) offers prospects for producing more reservoirs' original oil in place. As one of the most promising methods, chemical EOR (cEOR) is the process of injecting chemicals (polymers, alkalis, and surfactants) into reservoirs. However, the main issue that influences the recovery efficiency in surfactant flooding of cEOR is surfactant losses through adsorption to the reservoir rocks. This review focuses on the key issue of surfactant adsorption in cEOR and addresses major concerns regarding surfactant adsorption processes. We first describe the adsorption behavior of surfactants with particular emphasis on adsorption mechanisms, isotherms, kinetics, thermodynamics, and adsorption structures. Factors that affect surfactant adsorption such as surfactant characteristics, solution chemistry, rock mineralogy, and temperature were discussed systematically. To minimize surfactant adsorption, the chemical additives of alkalis, polymers, nanoparticles, co-solvents, and ionic liquids are highlighted as well as implementing with salinity gradient and low salinity water flooding strategies. Finally, current trends and future challenges related to the harsh conditions in surfactant based EOR are outlined. It is expected to provide solid knowledge to understand surfactant adsorption involved in cEOR and contribute to improved flooding strategies with reduced surfactant loss.

Keywords: Surfactant adsorption; Adsorption behavior; Influencing factors; Chemical additives; Chemical enhanced oil recovery.

Contents

Abstract 2

1. Introduction 4

2. Surfactant adsorption behavior 7

2.1 Mechanism of surfactant adsorption 7

2.2 Isotherms of surfactant adsorption 9

2.2.1 Langmuir adsorption isotherm 9

2.2.2 Freundlich adsorption isotherm 10

2.2.3 Temkim adsorption isotherm 10

2.2.4 Redlich-Peterson adsorption isotherm 11

2.3 Kinetics of surfactant adsorption 15

2.3.1 Pseudo-first-order kinetic model 15

2.3.2 Pseudo-second-order kinetic model 16

2.3.3 Intra particle diffusion kinetic model 17

2.3.4 Elovich kinetic model 18

2.4 Thermodynamics of surfactant adsorption 20

2.5 Structures of surfactant adsorption 22

3. Influencing factors on surfactant adsorption 26

3.1 Surfactant characteristics 26

3.2 Solution chemistry 31

3.3 Rock mineralogy 34

3.4 Temperature 36

4. Reducing surfactant adsorption 38

4.1 Alkalis 38

4.2 Polymers 40

4.3 Nanoparticles 43

4.4 Co-solvents and ionic liquids 46

4.5 Salinity gradient 47

4.6 Low salinity water flooding 48

5. Perspectives and challenges 49

6. Conclusions 52

Nomenclature 55

References 58

1. Introduction

With global oil demand and consumption forecast to rise continuously,[1] a realistic solution to fulfill this requirement is hinges on more efficient extraction of remaining oil from existing reservoirs.[2] Tertiary recovery or enhanced oil recovery (EOR) techniques offer prospects for generating more reservoirs' original oil in place (OOIP) which cannot be recovered using conventional recovery methods.[3] As one of the most promising EOR, chemical EOR (cEOR) has attracted much attention because of its higher efficiency, technical feasibility, economic viability, reasonable capital expenditures and with an additional 5-20% recovery at stake.[4–6] In cEOR, the injection of chemicals mainly includes surfactants, polymers, alkalis and formulated mixtures.[7–12] Owing to the existing synergies, these formulations have been normally screened in laboratory studies and each chemical influences the oil recovery by different mechanisms.[13] For example, application of polymers increases viscosity of the injected fluids and the oil/water mobility ratio, thus consequently enhances macroscopic displacement (volumetric sweep efficiency).[7,14] Introduction of surfactants is utilized to reduce the oil-water IFT, alter the mineral wettability, and contributes to the formation of micro emulsions, substantially improving the microscopic displacement efficiency.[4,15,16]

Most cEOR methods that have been developed are designed to increase the capillary number, N_c, defined as the ratio between viscous forces and capillary forces:[17]

$$N_c = \frac{\mu v}{\gamma \cos\theta} \tag{1-1}$$

where μ and v are the viscosity and velocity of the displacing liquid, γ is the oil-water IFT, and θ is the contact angle. As the capillary number (typically around 10^{-7} for water flooding) is increased,[11,18] the residual oil saturation will decrease, thereby augmenting recovery. This can be achieved by viscosity and velocity increases of the displacing liquid, a reduction in IFT, and/or rock wettability alteration. However, a significant increase in capillary numbers (10^{-4} to 10^{-2}) is required.[3,19] To obtain such high value, IFT needs to be reduced from the

initial high value of 20 – 30 mN/m to the order of 10^{-3} mN/m, by adding surfactants as the most feasible option.[20,21] Furthermore, the presence of surfactants can also drive the reservoir wettability towards a more water-wet state, promote the production of oil-water emulsions, and improve the interfacial rheological properties.[22–26] There are mainly two important aspects of interaction in cEOR: (1) fluid-fluid interaction where reservoir fluids (crude oil and brine) interact with the injection fluids,[27–31] (2) rock-fluid interaction where reservoir rock interacts with injection fluids.[32,33] For EOR optimization, both the phenomenon should be taken care while designing injection fluids and more specifically surfactant flooding.

The suitability of numerous surfactants in oil recovery has been evaluated and quantified in laboratory studies and field tests.[21,34,35] Technical screening criteria for surfactant flooding primarily include formation permeability, rock heterogeneity, solution chemistry (*i.e.* salinity, pH, and ions), reservoir temperature and depth, oil composition, and surfactant types and their structures.[21] Several reviews covering various features (fluid-fluid and rock-fluid interactions) of surfactant flooding have been reported. Belhaj et al. discussed the influence of surfactant concentration, salinity, temperature, and pH on surfactant adsorption for cEOR.[36] Kamal et al. reviewed different kinds of surfactants with particular emphasis on its phase behavior, adsorption, IFT, and field applications.[11] Zhang et al. summarized adsorption mechanisms and kinetics of surfactants and their mixtures at the solid-liquid interface.[37] Olajire reviewed the mechanisms, prospects, challenges of alkaline-surfactant-polymer (ASP) flooding, and status of ASP applications.[38] Bai et al. reviewed the recovery mechanisms of nanoparticle (NP) flooding and the synergistic effects of NP with surfactant nanofluids in cEOR applications.[39] Ahmadi et al. discussed the adsorption and thermal behavior of surfactants, phase behavior of emulsions, field trials of chemical assisted heavy oil recovery processes.[40] Hirasaki et al. analyzed recent developments to reduce the amount of surfactant required, mainly focusing on the role of alkali, alcohol, and chain branching.[41] From these

reviews, a key issue in surfactant flooding is the substantial loss of surfactants that reduces the recovery efficiency because of surfactant retention in porous media.

Surfactant retention is generally comprised of phase trapping, precipitation, and adsorption. The phase trapping and precipitation can be eliminated by appropriately selecting surfactants that are temperature and salinity tolerant, and adjusting relevant parameters (pH, formulations). However, surfactants are unavoidably adsorbed onto the rock surfaces and the impact of surfactant adsorption can be only mitigated. The adsorption takes place when the solid-liquid interface is energetically favored by surfactants compared to its bulk phase in the solution. Adsorption of surfactants on reservoir rocks has been determined usually using traditional depletion measurements (batch equilibrium tests on crushed core grains), and dynamic tests (core flooding experiments) by analyzing total surfactant content in effluents.[12,42–45] Research progresses in surfactant have also promoted a number of other techniques that can probe surfactants at interfaces to quantify the structure of the adsorbed surfactant film and monitor the kinetic adsorption processes.[46,47] For example, atomic force microscope (AFM) has considerably contributed to better understanding of dimensions, morphologies, and orientations of adsorbed surfactant layers.[48–52] More recently, quartz crystal microbalance with dissipation monitoring (QCM-D) has been applied to investigate the adsorption behavior of surfactants,[53–62] which can be also coupled with AFM, spectroscopic ellipsometry (SE), and surface plasmon resonance (SPR) techniques.[52,63–66] Therefore, to realize effective transport of surfactants into reservoirs, it is of great importance to understand surfactant adsorption on mineral surfaces.

In this review, the first section describes the adsorption behavior of surfactants, covering surfactant adsorption mechanisms, isotherms, kinetics, thermodynamics, and adsorption structures. The second section summarizes main factors affecting surfactant adsorption process such as surfactant characteristics, solution chemistry, rock mineralogy, and reservoir

temperature. Subsequently, different chemical additives of alkalis, polymers, nanoparticles, co-solvents, and ionic liquids are proposed to reduce surfactant adsorption, as well as salinity gradient and low salinity water flooding strategies. Finally, the upcoming trends and future challenges related to surfactant flooding at the harsh conditions are discussed.

2. Surfactant adsorption behavior

Surfactant adsorption to the reservoir rock is one of the most important parameters for chemical flooding. Adsorption means the loss of a valuable chemical component from solution, and as a consequence, a significant reduction of surfactant concentration in chemical slugs. Therefore, the efficiency of surfactant flooding will be substantially reduced not only in technical views (increase the oil-water IFT), but also in terms of the economic feasibility.[67–69] For good surfactant candidates, it should meet the requirements of low adsorption onto formation rock (<0.2 mg/g rock) and ultra-low IFT (10^{-3} – 10^{-2} mN/m).[20,70] In the surfactant-water-mineral system, numerous aspects of surfactant adsorption process have been discussed with particular emphasis on adsorption mechanisms, isotherms, kinetics, thermodynamics, and adsorption structures.

2.1 Mechanism of surfactant adsorption

Surfactant adsorption is a process where surfactant molecules are transferred from bulk solution to the solid-liquid interface through complex interactions between surfactant and rock surface. In general, surfactants adsorb on rock surfaces as monomers rather than micelles.[36] Adsorption is governed by a number of mechanisms, *i.e.*, electrostatic interactions (ion exchange/bridging), van der Waals interactions (London dispersion forces), acid-base interactions (hydrogen bonding, Lewis acid-base reactions), hydrophobic interactions, π electron polarizations, covalent bonding, and solvation of adsorbate species.[37,68,71–73] Several of the above mentioned mechanisms can contribute to the adsorption process, depending on the type of mineral and surfactant, surfactant concentrations, ionic strengths, and temperature.

Based on the formation rocks, oil reservoirs are typically classified into sandstones (silica) and carbonates (calcite and dolomite). The charge of a mineral surface is pH dependent, which can be positively or negatively charged by the dissociation/hydrolysis behavior of surface species or by the adsorption of ions/complexes in the aqueous solution. The isoelectric point (IEP) is the pH, at which a surface carries an average net charge of zero. When the pH is smaller than the IEP, the surface is positively charged. On the contrary, the surface has a negative charge at pH above the IEP. Silica has a IEP value of 2 – 3,[74–76] and the IEP of the most calcites is about 9.[77,78] Therefore, anionic surfactants tend to adsorb less to the silica surface because it is negatively charged at reservoir pH (5 – 9) that is larger than IEP of silica, whereas cationic surfactants are preferentially attracted.

The added alkalis are not only to raise the solution pH, but also render more negative mineral surfaces, leading to a considerable reduction of anionic surfactant adsorption because of electrostatic repulsions.[79] The electrostatic interaction plays a prominent role between the charged head of ionic surfactants and the rock surface.[80,81] Calcium cation bridging is of great importance to bind anionic surfactant to the negatively charged clay surface.[53] Adsorption by London dispersion forces usually increases with increasing the molecular weight (MW) of surfactant.[72] When surfactant molecules comprise functional groups such as hydroxyls, carboxylates, amines and phenols, the adsorption process could occur through hydrogen bonding interactions.[82] The hydrophobic interaction mainly takes place when the alkyl chain of a surfactant adsorbs on fully or partially hydrophobic surfaces, or surfactant layer by layer adsorption (formation of hemi-micelles, admicelles) via hydrophobic chain-chain interactions.[37] Adsorption by π electron polarization occurs when the surfactant has an electron-rich aromatic nucleus and the rock surface contains highly positive sites.[72] In addition, chemical bonding is another driving force resulting in the adsorption (chemisorption) of oleate ions and oleic acid amides on apatite by the formation of Ca-O/N bonds.[83] When

hydrated head groups of surfactants adsorb on the solid-liquid interface, water molecules in the secondary solvation shell around head groups can be partially removed. In comparison to other interaction mechanisms, the possible dehydration process of ionic head groups of surfactant is unfavorable for adsorption.[37]

2.2 Isotherms of surfactant adsorption

At constant temperature, the adsorption isotherm is applied to evaluate the relationship between the amount of surfactant adsorbed at a solid-liquid interface and the initial surfactant concentration in solution after equilibrium is reached. This is important to assess the amount of surfactant loss through adsorption to the rock surface. Four well-known adsorption isotherms have been commonly used to characterize the adsorption equilibrium behavior for surfactants, which are briefly described below.

2.2.1 Langmuir adsorption isotherm

The Langmuir isotherm model assumes that monolayer adsorption occurs on the uniform surface of a fixed number of well-defined sites, with no interactions between adsorbed surfactants.[84,85] Each site is energetically equivalent, and can only accommodate one surfactant molecule.[86] The Langmuir equation is represented by:

$$q_e = q_m \frac{K_L C}{1+K_L C} \quad (2.2\text{-}1)$$

where q_e, q_m, and C, are the equilibrium adsorption, maximum amount of surfactant adsorption, and equilibrium surfactant concentration, respectively. K_L is the Langmuir equilibrium constant associated with the adsorption energy. The Langmuir equation can be converted into a linearized form:

$$\frac{1}{q_e} = \frac{1}{q_m} + \frac{1}{C} \cdot \frac{1}{q_m K_L} \quad (2.2\text{-}2)$$

From the plot of $1/q_e$ versus $1/C$, K_L and q_m can be derived from the slope and intercept, respectively. To represent the compatibility of adsorption, the non-dimensional constant R_L is defined as $R_L = 1/(1 + K_L C_0)$. Here, C_0 is the initial adsorbate concentration. The lower R_L is,

more favorable adsorption will be. The R_L is found to be always no larger than unity, and thus the adsorption is favorable.[45,87,88] The Langmuir adsorption isotherm (L-type) features a continuous and monotonous decrease in adsorption rate because vacant adsorption sites decrease as the adsorbent becomes covered. Many surfactant adsorption data have shown a good fit to the Langmuir equation,[12,44,45,89,90] but the assumptions of the Langmuir model are not fulfilled, particularly in the absence of lateral interactions. There are several mutual compensation factors influence the final shape of the Langmuir isotherm, such as adsorption of micelles, inhomogeneous surface potentials, surface impurities, lateral interactions between surfactant molecules.[91]

2.2.2 Freundlich adsorption isotherm

The Freundlich isotherm is an empirical model to evaluate non-ideal and reversible adsorption processes (*e.g.*, surfactant multilayer adsorptions onto heterogeneous surfaces). At various solute concentrations, the ratio of adsorbed solutes to the solute concentration is not a constant.[92] As a result, this isotherm is unable to estimate saturations of adsorbents by the adsorbates; thus, infinite surface coverage is presumed mathematically, suggesting a multilayer adsorption on the surface.[93] In the Freundlich isotherm, the adsorbed amount is proportional to the surfactant concentration to the power 1/*n*:

$$q_e = K_F C^{1/n} \quad (2.2\text{-}3)$$

where K_F is the Freundlich constant related to the capacity of adsorption and n is a heterogeneity factor. It is assumed that there are various types of adsorption sites on the inhomogeneous surface, which make it possible to describe multilayer adsorption.[44] Taking the logarithm of Γ and plotted versus log(C), n and K_F can be derived from the slope and intercept of the straight plot, respectively. It is found that 1/n is no larger than 1, indicating favorable adsorption of the system.[12,94]

2.2.3 Temkim adsorption isotherm

Indirect interactions of adsorbate-adsorbate are considered in the Temkin isotherm. On account of these interactions and ignoring too low and too high solute concentration values, the heat of adsorption of all molecules in the adsorbed layer will decrease linearly with coverage of the solid surface with surfactant. This adsorption is illustrated with a homogeneous distribution of binding energy, up to some maximum binding energies.[95] The isotherm model is given by the following equation:

$$q_e = BlnK_T + BlnC \quad (2.2\text{-}4)$$

where K_T denotes the Temkin constant and B is a constant related to the heat of adsorption. By plotting the quantity adsorbed q_e against lnC, the constants B and K_T are determined from the slope and intercept of a straight plot. This isotherm fails to predict the experimental data when the relationship between rock surface coverage and adsorption heat of surfactants is logarithmic rather than linear.

2.2.4 Redlich-Peterson adsorption isotherm

The Redlich-Peterson isotherm is applied as a compromise between the Langmuir and Freundlich isotherms. This model is an empirical isotherm comprising three different parameters. Therefore, the adsorption mechanism is complicated and does not follow the assumption of ideal monolayer adsorption. It is represented by the following equation:

$$q_e = \frac{K_R C}{1+BC^{\beta}} \quad (2.2\text{-}5)$$

where K_R and B are the Redlich-Peterson constants. β is the exponential constant that lies between 0 and 1, which can help to characterize the adsorption isotherm model. When β = 1, *eq.*(2.2-5) is reduced to the Langmuir equation with $B = K_L$ and $K_R = K_L * q_m$; When β = 0, *eq.*(2.2-5) condenses to the linear isotherm model with 1/(1 + B) representing Henry's constant. Henry's equation presents linear adsorption isotherm behavior only at lower concentrations.[86] At high surfactant concentrations, *eq.*(2.2-5) is reduced to the Freundlich equation:

$$q_e = \frac{K_R}{B} C^{1-\beta} \quad (2.2\text{-}6)$$

Where K_R/B equals to K_F and (1- β) = 1/n of the Freundlich isotherm model. Taking a natural logarithm on both sides of *eq.*(2.2-5), the Redlich-Peterson isotherm is rearranged into a linearized form as follows:

$$ln\left(K_R \frac{C}{q_e} - 1\right) = \beta lnC + lnB \quad (2.2\text{-}7)$$

To obtain a linear plot of *eq.*(2.2-7), various constant K_R values should be tried, from 0.01 to several hundred.[96] In the adsorption of soap-nut surfactant, the interactions were complex and various intermolecular forces existed, such as electrostatic attractions, hydrogen bonding, covalent bonding, and hydrophobic interactions.[97] Compared to the above mentioned four isotherm models, the adsorption pattern of soap-nut surfactant was better fitted with the Langmuir model as well as with the Redlich-Peterson adsorption isotherm that supported the monolayer adsorption behavior.[98]

Apart from these four equilibrium models commonly described, other models are included and summarized in **Table 1**, which can be utilized to clarify how an adsorbate is adsorbed onto an adsorbent.[99,100]As surfactant adsorption is strongly temperature dependent, isotherm models are necessary to be used at different temperatures. The model possessing the best values of coefficient of determination (R^2) and the lowest values of standard deviation (*SD*) for a majority of temperatures should be rated as the best isotherm model. For example, in comparisons to the Freundlich and Tempkin models, very high R^2 coefficients for the adsorption of the different surfactants were obtained with the Langmuir model.[89]

Table 1. Lists of adsorption isotherms models.[82,84,99,100]

Parameter	Isotherm model	Nonlinear form	Linear form
One	Henry	-	$q_e = K_H \cdot C$
Two	Langmuir	$q_e = q_m \frac{K_L C}{1 + K_L C}$	$\frac{1}{q_e} = \frac{1}{q_m} + \frac{1}{C} \cdot \frac{1}{q_m K_L}$
	Freundlich	$q_e = K_F C^{1/n}$	$\log q_e = \log K_F + 1/n \log C$
	Temkin	$q_e = BlnK_F C$	$q_e = BlnK_T + BlnC$
	Dubinin-Radushkevich	$q_e = q_m e^{-K_D \varepsilon^2}$	$lnq_e = lnq_m - K_D \varepsilon^2$
	Elovich	$\frac{q_e}{q_m} = K_E C e^{\frac{q_e}{q_m}}$	$\ln \frac{q_e}{C} = lnK_E q_m - \frac{q_e}{q_m}$
	Jovanovic	$q_e = q_m(1 - e^{K_J C})$	$lnq_e = lnq_m - K_J C$
Three	Redlich-Peterson	$q_e = \frac{K_R C}{1 + BC^{\beta}}$	$ln\left(K_R \frac{C}{q_e} - 1\right) = \beta lnC + lnB$
	Sips	$q_e = \frac{K_S C^{\beta}}{1 + \alpha_S C^{\beta}}$	$\beta lnC = -\beta ln \frac{K_S}{q_e} + ln\alpha_S$
	Toth	$q_e = \frac{K_T C}{(\alpha_T + C)^{1/t}}$	$ln \frac{q_e}{K_T} = lnC - \frac{1}{t} ln(\alpha_T + C)$
	Koble-Carrigan	$q_e = \frac{AC^n}{1 + BC^n}$	$\frac{1}{q_e} = \frac{1}{AC^n} + \frac{B}{A}$
	Radke-Prausnitz	$q_e = \frac{q_m K_R C}{(1 + K_R C)^n}$	$ln \frac{q_e}{q_m K_R} = lnC - nln(1 + K_R C)$

However, not all surfactant adsorption isotherms follow a specific model. **Figure 1** shows a typical four-region (S-type) adsorption isotherm in an extensive range of surfactant concentrations going beyond the critical micelle concentration (CMC).[101,102] Adsorption in various regions was explained by taking considerations of electrostatic, hydrophobic and micellar interactions. In region I, surfactant adsorption is primarily by electrostatic interactions by the head groups of surfactant monomers in contact with the mineral surfaces and its alkyl tails pointed outwards. At low surfactant concentration, the adsorption process

obeys Henry's law, and the adsorbed amount increases linearly with the surfactant concentration.[103] In region II, a substantial increase in the adsorption results in the formation of hemimicelles due to lateral interactions between the alkyl tails of the adsorbed monomers. Otherwise, the electrostatic interaction is still active at this stage. In the end of the region II, the surface is electrically neutralized by the adsorbed surfactants. Further adsorption in region III occurs by chain-chain hydrophobic interactions alone, showing a slower adsorption rate than region II because less adsorption sites are present. Above the CMC in region IV, the monomer concentration of surfactants is approximately constant, and any increase of surfactant concentrations only works for more micelles, which does not affect the maximum adsorption. The adsorption isotherm of sodium dodecyl sulfate (SDS) on alumina surface exhibited an S shape adsorption isotherm with a four-stage adsorption process.[101] Sometimes only three different stages are found in the adsorption isotherms and region III is not clearly identified. This can be attributed to comparable slopes for regions II and III, which are observed on loose packing of the cationic surfactant aggregates.[104] The adsorption of alkyl trimethylammonium vinylbenzoate (CTVB) onto silica surface showed a two/three-stage adsorption isotherm, depending on the length of hydrocarbon tail.[105] Many descriptions of two-step isotherms are also available for a wide variety of surfactant adsorption.[40,106,107] Obviously, these models have a good deal in common and the main difference is a lack of hydrophobic interaction in the second region for the two-step model.

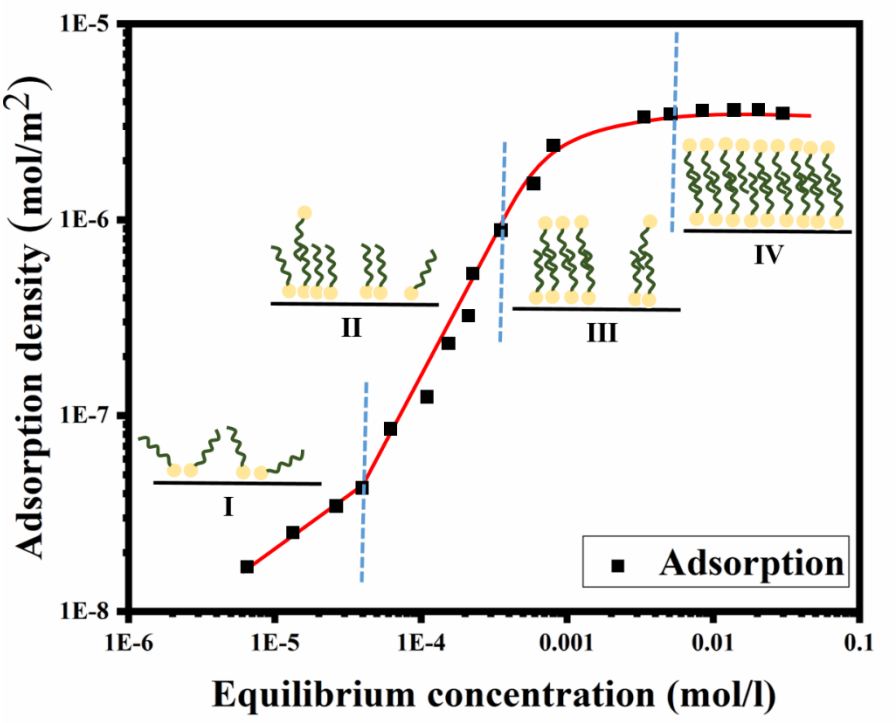

Figure 1. Schematic representation of the typical four-region (S-type) adsorption isotherm. Reproduced from Somasundaran and Zhang.[101]

2.3 Kinetics of surfactant adsorption

Modeling of the kinetics of surfactant adsorption is as important as the adsorption isotherm. It describes both the diffusive transport of surfactant molecules from the bulk solution to the liquid-solid interface and the kinetics taking place at the interface itself. Adsorption kinetics are available to determine the adsorption rate versus time and give useful information about mechanisms of the adsorption. The following sections summarize four widely used adsorption kinetic models to evaluate adsorption processes.

2.3.1 Pseudo-first-order kinetic model

A first-order rate equation to elucidate the kinetic process of liquid-solid phase adsorption was initially established by Lagergren,[108] which shall be deemed to be the earliest model concerning the adsorption rate by means of the adsorption capacity. It is assumed that the occupation rate of adsorption sites is proportional to the number of available sites. The differential formulation of the addressed kinetic model is given by:

$$\frac{dq_t}{dt} = K_1(q_e - q_t) \quad (2.3\text{-}1)$$

where q_t is the amount of surfactant adsorbed at time *t*, and K_1 is the equilibrium rate constant of pseudo-first-order (PFO) adsorption. The integral of *eq.*(2.3-1) with the boundary condition of $q_t = 0$ at t = 0 and q_t = t at t = t yields a linear expression[109,110]:

$$ln(q_e - q_t) = lnq_e - \frac{K_1}{2.303}t \quad (2.3\text{-}2)$$

The value of K_1 is determined by the slope of the linear plot of *ln* (q_e-q_t) versus t. The *eq.*(2.3-2) can be rewritten as:

$$q_t = q_e\left(1 - e^{-\frac{K_1}{2.303}t}\right) \quad (2.3\text{-}3)$$

To fit the above given equations with the experimental data, it is essential to acquire the value of q_e. It can be possible that the amount adsorbed is considerably lower than the actual equilibrium amount after a long interaction time.[111] The value of K_1 is usually inversely proportional to the initial adsorbate concentration.[112] The validity of *eq.*(2.3-2) arises from the comparison of as-calculated q_e to the experimentally determined q_e. For many adsorption processes, the PFO model is generally applicable for the early interaction time of 20 to 30 min and is not suitable for the whole period.[113]

2.3.2 Pseudo-second-order kinetic model

A pseudo-second-order (PSO) model is obtained based on the adsorption capacity of the solid phase, represented as[114]:

$$\frac{dq_t}{dt} = K_2(q_e - q_t)^2 \quad (2.3\text{-}4)$$

where K_2 is equilibrium rate constant of PSO model and is similar to PFO model. Integrating *eq.*(2.3-4) with the boundary condition ($q_t = 0$ at t = 0 and q_t = t at t = t) gives:

$$\frac{t}{q_t} = \frac{1}{K_2 q_e^2} + \frac{t}{q_e} \quad (2.3\text{-}5)$$

The intercept of the linear plot of t/q_t versus *t* and its slope are acquired to extract the equilibrium rate constant K_2 and adsorption amount q_e. Even though the PSO model can be

affected by applied solution pH, surfactant concentration, and temperature, the model evaluates the influence of observable rate parameters. The initial adsorption rate (h) and half-adsorption time ($t_{1/2}$) are acquired by the following equations:

$$h = K_2 q_e^2 \quad (2.3\text{-}6)$$

$$t_{1/2} = \frac{1}{K_2 q_e} \quad (2.3\text{-}7)$$

This PSO model has been successfully employed to examine the adsorption kinetics of metal ions, herbicides, dyes, oils, and organic materials from aqueous solutions.[40] When the solute concentration is not too high, PSO model is favored; On the contrary, PFO fits better at a higher the solute concentration.[115] In most cases, PSO model shows a wide applicability over PFO, and the obtained q_e with PSO is close to the experimental value, with much higher degree of correlation.[112,116] However, the ability of a model to fit experimental data is not enough to prove the validity of the underlying mechanism.[109] Both PSO and PFO models are useful to figure out the reaction types and rate constants, but do not explain the adsorption process controlled by diffusion; thus, before any conclusions can be drawn about adsorption mechanisms, diffusion models should be examined as well.

2.3.3 Intra particle diffusion kinetic model

With the purpose of determining distinct diffusion processes such as internal and external diffusion mechanisms, the intra particle diffusion (IPD) equation is proposed[110,117]:

$$q_t = K_i t^{1/2} + c \quad (2.3\text{-}8)$$

where K_i is equilibrium rate constant of IPD model, and c is a constant associated with the adsorption step. A linear plot of q_t versus $t^{1/2}$ calculates constant K_i. K_i generally increased with increasing initial adsorbate concentration.[118] If the plot passes through the origin (zero intercept), IPD dominates the adsorption process. However, it sometimes shows multilinearity over the entire adsorption process. Multilinearity is an indication of multiple adsorption mechanisms, such as mass transfer, film diffusion, surface diffusion, and pore

diffusion.[119] Each linear segment represents one or more controlling mechanisms. A typical three stages proceed by surface adsorption by boundary layer diffusion, intra particle diffusion, and a likely chemical reaction stage. Among these steps, the last step is very rapid and considered to be negligible.[120] Determining how many linear segments and the time period for each line segment the adsorption process are somewhat arbitrary. The use of piecewise linear regression can be helpful for analyzing adsorption data by IPD model.[121]

2.3.4 Elovich kinetic model

The Elovich equation neglects desorption and is applied to determine the chemisorption kinetics, which can also to evaluate the mass and surface diffusions, activation and deactivation energies of a system. It has been assumed that the adsorption rate declines exponentially with the increasing amounts of adsorbed solutes.[114] The kinetics relationship is described by the Elovich equation:

$$\frac{dq_t}{dt} = \alpha e^{-\gamma_1 q_t} \quad (2.3\text{-}9)$$

where α the initial adsorption rate, and γ_1 is the desorption constant associated with the extent of surface coverage and activation energy for chemisorption. With the assumption of $\alpha\gamma_1 t >> 1$, *eq.*(2.3-9) was integrated by using the boundary condition (q_t = 0 at t = 0 and q_t = t at t = t), the Elovich model is linearized as:

$$q_t = \frac{1}{\gamma_1}\ln(\alpha\gamma_1) + \frac{1}{\gamma_1}\ln(t) \quad (2.3\text{-}10)$$

The graph of q_t versus *ln(t)* is used to assess the adsorption nature on the heterogeneous surface, whether chemisorption or not. The Elovich equation neglects desorption due to chemisorption that is physically unsound as an infinite q_t would be at long periods of adsorption.[122] Thus, the range of Elovich model application is limited to the initial adsorption process, when the system is rather far from equilibrium.[123] When the fractional surface coverage is lower than around 0.7, the Elovich model is essentially identical to the PSO model.[124]

Table 2. Summary of four adsorption kinetic models.

Kinetic model	Equation	Application conditions	Examples
Pseudo-first-order (PFO)	$\frac{dq_t}{dt} = K_1(q_e - q_t)$	PFO model is valid only under either of these two sets of conditions (i) reaction control and Henry regime adsorption, or (ii) reaction control and high adsorbent dose.[125] For many adsorption processes, the PFO model is found suitable only for the initial 20 to 30 min of interaction.[113]	PFO model can best predict the kinetic process of Congo red adsorption from aqueous solutions using cationic surfactant modified wheat straw.[126]
Pseudo-second-order (PSO)	$\frac{dq_t}{dt} = K_2(q_e - q_t)^2$	Most environmental kinetic adsorption can be modelled well by PSO, when the solute concentration is not too high.[108] In most cases, PSO model shows a wide applicability over PFO.	The kinetics of Saponin surfactant adsorption on the shale sandstone were persuasively estimated with the PSO model.[86]
Intra particle diffusion (IPD)	$q_t = K_i t^{1/2} + c$	Multi-linearity nature in adsorption of the surfactant is emerged, indicating of multiple adsorption mechanisms, such as mass transfer, film diffusion, surface diffusion, and pore diffusion.[86]	The results matched well with PSO and IPD model suggests that the adsorption process proceeds by surface sorption and intra-particle diffusion.[127]
Elovich	$\frac{dq_t}{dt} = \alpha e^{-\gamma_1 q_t}$	Assuming strong heterogeneity at the adsorbent surface, it is suitable for kinetics far from equilibrium and describes chemisorption well.[123]	When the dodecylamine is mainly in the form of micelle or precipitation, the initial rapid stage is best fitted by the PFO model, while the second stage is best fitted by the Elovich model.[57]

Although the list of kinetic models presented above is by no means comprehensive,[123,125] they are frequently used for surfactant adsorption (Table 2). In the study of DICL adsorption, Kou and Xu fitted the adsorption data with PFO, PSO, and Elovich models.[57] When the DICL was predominantly ion or molecular forms at pH 5.7, PSO model showed the best fit to the only one adsorption stage; when the DICL micelle was adsorbed, there were two different adsorption stages, the first fast stage was best described by PSO model and the second one can be best described by the Elovich model.[57] Such adsorption process cannot be simply fitted using a single kinetic model, and they are better described by two or three simultaneous models.[128] Chen et al. characterized a two-step adsorption of a switchable cationic surfactant using QCM-D, with a fast adsorption of surfactants with its head groups orientated toward silica surfaces, succeeded by a slow process in line with the formation of surfactant aggregations, *ie.*, bilayered admicelles.[60] Impact of surface roughness on cetyltrimethyl ammonium bromide (CTAB) adsorption kinetics were also found, implying the presence of more high energy sites on the rougher surface.[129] The adsorbed amount of polymer-surfactant mixtures showed a $t^{1/2}$ dependence within the experimental error for $t \rightarrow 0$, which was typical for a diffusion controlled kinetics.[130] The rate of adsorption and desorption can be derived from the linear dependence of equilibrium rate constant on surfactant concentration with PFO and PSO models. A higher adsorption to desorption ratio indicated the overall adsorption reaction was more delocalized to surfactant adsorption, such as the fouling potential of sodium dodecylbenzene sulfonate (SDBS) on titania.[58]

2.4 Thermodynamics of surfactant adsorption

In an effort to estimate the effect of temperature on the adsorption, thermodynamic considerations regarding an adsorption process are essential to determine whether the process is spontaneous. Gibbs free energy change (ΔG°) is a key parameter for identifying the spontaneity of a process. If ΔG° becomes negative, the adsorption process occurs

spontaneously at a given temperature. Generally, ΔG° is in the range of 0 to -20 kJ/mol for the physical adsorption, and -80 to -400 kJ/mol for the chemisorption.[131] Considering the changes in the equilibrium constant (K°) at various temperatures, ΔG° could be obtained from the Van't Hoff equation as follows[132–134]:

$$\Delta G^{\circ} = -RT\, lnK^{\circ} \quad (2.4\text{-}1)$$

where T is absolute temperature in Kelvin (K), and R is the universal gas constant (8.314 $J\ mol^{-1}K^{-1}$). The entropy (ΔS°) and enthalpy (ΔH°) are two important parameters in the feasibility and spontaneity of a process that is related to ΔG°, defined as

$$\Delta G^{\circ} = \Delta H^{\circ} - T\Delta S^{\circ} \quad (2.4\text{-}2)$$

ΔG° can be always negative in the case of entropy is positive ($\Delta S^{\circ} > 0$) and enthalpy is negative ($\Delta H^{\circ} < 0$), indicating a spontaneous adsorption process at all temperatures. A negative ΔH° refers to an exothermic adsorption process, while a positive ΔS° implicates the increased degree of freedom (randomness) of the adsorbate towards solid-liquid interface and more favorable condition for the occurrence of the adsorption process. Combing *eq.*(2.4-1) and (2.4-2), it leads to:

$$ln\, K^{\circ} = \frac{\Delta S^{\circ}}{R} - \frac{\Delta H^{\circ}}{R}\frac{1}{T} \quad (2.4\text{-}3)$$

Using a plot of $1/T$ versus $\ln(K^{\circ})$, the values of ΔH° and ΔS° could be acquired from the slope and the intercept, respectively. The calculation of K° is derived by fitting the adsorption isotherms at various temperatures in Section 2.2. It should be noted that the obtained $K^{\circ'}$ (usually expressed in L/mg) in the isotherms need to be dimensionless for being applied in the Van't Hoff equation. Converting the units of obtained $K^{\circ'}$ to dimensionless K° can be[134]:

$$K^{\circ} = \frac{(1000 \cdot K^{\circ'} \cdot molecular\ weight\ of\ adsorbate)\ [adsorbate]^{\circ}}{\tau} \quad (2.4\text{-}4)$$

where τ (dimensionless) is the activity coefficient, and [adsorbate]° (1 mol/L) is the standard adsorbate concentration. For this conversion, the adsorbate solution is very diluted and

therefore the activity coefficient is one.[132] After making these calculations, the parameter K° becomes dimensionless.

Using the Langmuir isotherms with the above formulae, the values of ΔG° at different temperatures are negative and hence the adsorption of nonionic surfactants is spontaneous, while the negative ΔH° confirmed that the adsorption process is exothermic.[45] Thus, the increasing temperature decreased the adsorption of nonionic surfactants on carbonate surfaces. The calculated ΔG° indicated the adsorptions of phenols were mainly physical in nature and were strengthened by chemisorption and the negative ΔH° demonstrated the exothermic nature of these phenol adsorptions, which were consistent with experimental observations.[135] The adsorption of SDS surfactant on the Algerian rock specified the feasibility, spontaneity, and exothermic nature of the adsorption process.[85] With an increase in temperature, the adsorption of SDS surfactant on sand surface decreased as the randomness of the molecules at the solid-liquid interface decreased.[12] An exothermic adsorption of a natural surfactant derived from leaves of Zyziphus Spina Christi on shale-sandstone reservoir rocks was observed on both static adsorption and core flooding experiments.[86] However, these obtained thermodynamic parameters of ΔG°, ΔS° and ΔH° directly used $K^{\circ,}$ rather than dimensionless K°. Recently, Lima et al. revealed the wrong use of equilibrium constants in the Van't Hoff equation for calculations of thermodynamic parameters of the adsorption.[134] Therefore, the use of Van't Hoff equation should be careful to ensure dimensionless, as an estimative of thermodynamic parameters.

2.5 Structures of surfactant adsorption

An understanding of the structure that surfactants adsorbed at rock surfaces is vital to determine their roles in cEOR. AFM is particularly well suited to obtain high-resolution nanoscale images of surfactant adsorbed films. Kou et al. observed that DICL colloids were adsorbed or precipitated onto the surface, giving rise to porous and heterogeneous multilayer

structures.[57] The adsorption of polymer-surfactant complexes resulted in inhomogeneous films formed by isolated aggregates randomly distributed through the surface.[130] The addition of a gemini surfactant to the monomeric surfactant triggered dramatic shape transition in the adsorbed layer morphology among circular aggregates, worm-like aggregates, and lamellar bilayer.[50] At a concentration of 1.2 × CMC, the CTAB adsorbed layer exhibited prolonged rod-like micelles with the mean spacing of 9 nm, whereas dodecyltrimethylammonium bromide (DTAB) showed small micellar aggregates with the mean spacing of 5 – 6 nm, as shown in **Figure 2**.[136] Moreover, the force-distance data acquired from AFM measurements gain further insights into the adsorbed structure. The attractive interaction between CTAB and AFM tips reflected the likely formation of hemimicelles on the silica surface.[137] The breakthrough distance in the force-distance curve offers a measure to the adsorbed layer thickness, and the breakthrough force represents the force needed to penetrate the adsorbed layer to the underlying substrate.[48,138] A surface aggregate thickness of CTAB was determined to be ~1.0 nm.[139] Two force instabilities have been pointed out due to the collapse of the surfactant layer weakly bound onto the tip at long-range separations, followed by short-range repulsion force from surfactant aggregates evolved on the surface.[140] Recently, high-speed AFM (HS-AFM) shows the potential to capture the dynamics occurring at the solid-liquid interface. Inoue et al. recorded the adsorption kinetics of a cationic surfactant (hexadecyltrimethyl ammonium chloride, CTAC) on the mica surface.[141] At 2 × CMC of CTAC, worm-like and cylindrical micelles were found after 10 to 30 s, which then changed into a bilayer after about 300 s. The solubilization-induced morphological transformation in CTAB aggregates was visualized using HS-AFM.[52]

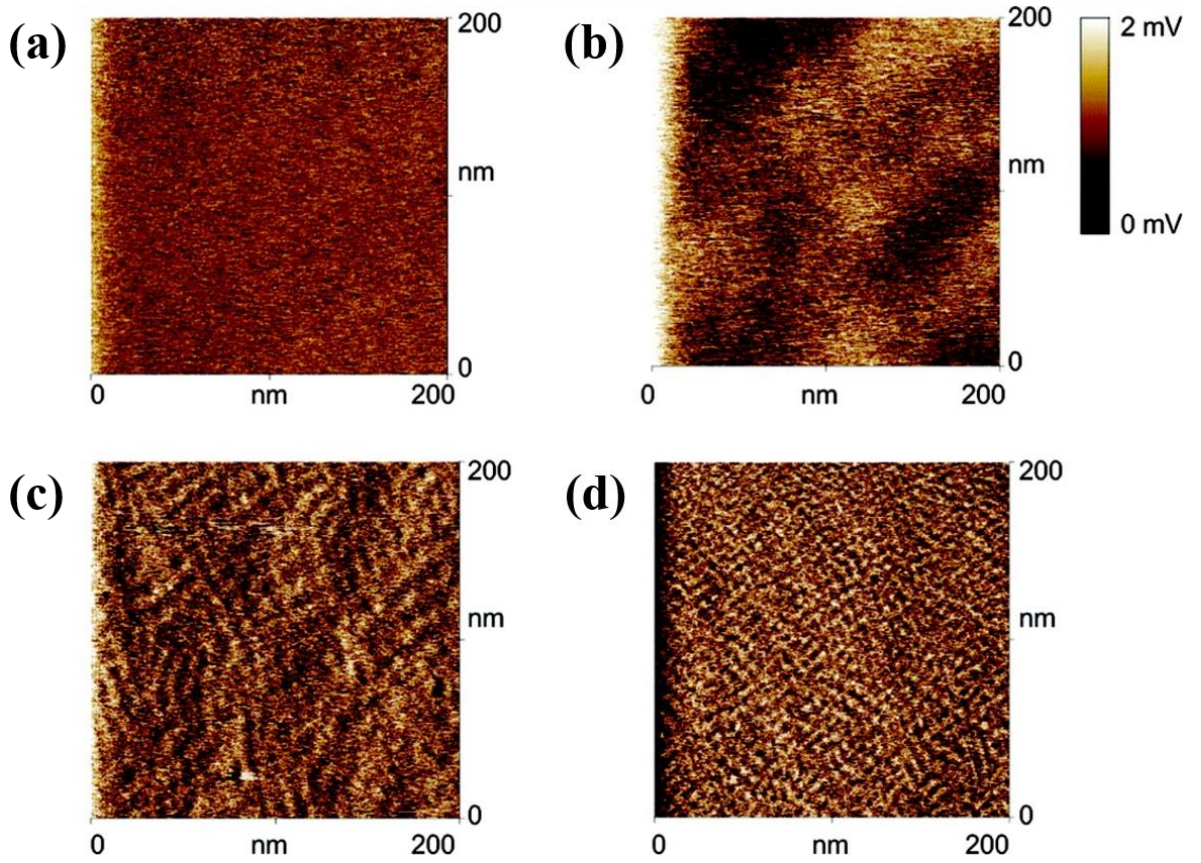

Figure 2. AFM images of (a) bare SiO_2 showing no features, (b) an adsorbed layer of DDAB showing large scale undulations, (c) an adsorbed layer of CTAB showing prolonged rod-like micelles, with an average spacing of ~9 nm, and (d) an adsorbed layer of DTAB showing small micellar aggregates with an average spacing of ~5 – 6 nm. Reprinted with permission from.[136]

SE is capable to detect small changes in the refractive index of the adsorbed layer, and provides complementary information regarding the adsorbed amount to QCM-D. It has been observed that the water content increased with increasing concentration of an amphiphilic polyelectrolyte (acryloyloxyethyl-N, N-dimethyl-N-octylammonium bromide, PASC8), and then reaches a plateau of about 20% water, indicating a tight and dense structure related to containing more water, which was driven by both of the electrostatic and hydrophobic interactions.[142] The micelle-assisted CTAB film growth revealed an undulated surface with rod-like and sphere-like distorted bilayer structures and defect boundary regions.[143] The correlation of SE and QCM-D data can provide novel insight, that is not available with either technique alone. A central parameter is solvation (or porosity or trapped solvent) that is accessible for ultrathin adsorbed layer up to a few nm, or can be resolved with significantly

improved precision for films of intermediate thickness up to a few 10 nm.[63] Another optical technique to investigate the surfactant adsorption is SPR, but limits to the surface with a plasmon band, typically on the metal surface. The weak dependence of SPR signal on the conformation, molecular weight, etc., renders the mass estimation extremely convenient, whereas the strong sensitivity of the intrinsic viscosity to these factors complicates the accurate mass calculation with QCM-D.[144]

Although other spectroscopic techniques are reported, they are not frequently used and are briefly summarized below. Neutron reflectivity allows us to broaden investigations into the structural detail of adsorbed layers, as different nuclei scatter neutrons with different amplitudes,[145–147] and offers a comprehensive description of the mean surfactant concentration profile normal to the surface at equilibrium.[148] A surfactant mixture, containing two or more surfactants, can be studied using solid-state proton nuclear magnetic resonance spectroscopy, either individually if there are unique peaks for each surfactant or all together if the peaks are overlapped.[149] Moreover, the total internal reflection Raman scattering (TIR Raman) and sum-frequency spectroscopy (SFS) have been employed to investigate the adsorption of CTAB on hydrophilic silica surface, and the average orientation and packing of the hydrocarbon chains of CTAB were irrelevant to surface coverages.[150] TIR Raman also explored adsorption and desorption kinetics of surfactants at the solid-liquid interface.[151] SFS gained a better understanding of the mechanisms and kinetics of surfactant monolayer self-assembly on the fluorite surface.[152]

In support of experiments, both atomistic and coarse grain molecular dynamics (MD) simulations have been assisted in understanding how surfactants adsorb on rock surfaces. It can predict how every atom in a surfactant or molecular systems will move and interact over time, giving a view of the dynamic evolution of the surfactant system. Various morphologies of adsorbed SDS were observed on silica with varying degrees of hydroxylation and charge

densities using MD simulations.[153] The aggregate morphology of dual-tailed surfactants yielded bilayer structures on alumina.[154] As the increase in CTAB concentration, single and small groups of surfactant molecules were found to lie on the silica, hemimicelles, and micelles.[155] Sammalkorpi et al. revealed that point (*i.e.*, vacancies) and line (*i.e.*, surface steps) defects influenced the stability and orientation of SDS aggregates.[156] By applying dissipative particle dynamics (DPD) simulations, the morphology of surfactant aggregations heavily depended on the surface morphologies and chemical heterogeneities.[157,158] MD studies of the adsorption of pure and mixed surfactants on muscovite surface showed good agreements with experimental results.[159] To select an optimal surfactant molecule, Li et al. modelled oil detachment process in the presence of different surfactants.[160] Simulation studies are also capable to estimate several fundamental properties in the surfactant-rock system such as surface activities, contact angles, and adsorption isotherms. Molecular level information, obtained from both experiments and simulations, are important to achieve the improved understanding of the surfactant adsorption process.

3. Influencing factors on surfactant adsorption

Surfactant adsorption is considered as a negative impact that is disadvantageous for improving surfactant flooding efficiency and can reduce technical and economic competitiveness of surfactants. Thus, a comprehensive knowledge of factors affecting surfactant adsorption is highly significant before the coming injection of surfactant slugs for cEOR. In surfactant-water-rock systems, main factors including surfactant characteristics (*i.e.*, structure, concentration), solution chemistry (*i.e.*, salinity, ionic composition, and pH), rock chemistry (*i.e.*, rock type, impurities, roughness), and reservoir temperature (increasing with depth) that have a serious impact on surfactant adsorption are thoroughly discussed.

3.1 Surfactant characteristics

According to the nature of hydrophilic head groups, surfactants are majorly divided into four classes: anionic, cationic, zwitterionic, and nonionic surfactants (**Figure 3**). Anionic surfactant is the most commonly used type, containing sulfate ($-O-SO_3^-$), sulfonate ($-SO_3^-$), or carboxylate ($-COO^-$) groups, though usually in association with an alkaline metal (Na^+ or K^+) cation. The sulfate surfactant has a better tolerance to salinity for both monovalent and divalent cations, but can be easily decomposed at temperature higher than 60 °C. On the other hand, surfactants containing sulfonate groups are tolerated to high temperature, but sensitive to high salinity and easily precipitate at high divalent cation concentrations.[11,80,161] The most commonly used surfactants for cEOR are sulfonate surfactants, which were produced either by direct sulfonation of aromatic groups in refinery streams or crude oils, or by organic synthesis of alkyl/aryl sulfonates.[41] Petroleum sulfonate, synthetic alkyl/aryl sulfonate, internal olefin sulfonate (IOS), alpha olefin sulfonate (AOS), and alkoxy sulfonates have been evaluated for cEOR applications.[11,161] Equilibrium adsorption for the alkyl aryl sulfonate surfactant was 3.5 mg/m^2, whereas its ethoxylated counterpart demonstrated lower adsorption of 0.8 mg/m^2 on calcite.[162] Under water-wet conditions, changing the surface redox potential from an oxidized to a reduced state decreased the $C_{14–16}$ AOS adsorption level by 40%, to ~0.3 mg/g on Berea sandstone cores.[163] At a concentration of 3000 ppm of IOS, increasing the pH from 8.24 to 9.57 decreased surfactant adsorption from 0.760 to 0.161 meq/100 g of rock.[164] Adsorption of $C_{15–18}$ IOS onto two pure minerals (calcite and quartz) are about the same ~1.1 mg/g, and the adsorption capacity of shales depends on the mineral composition, ranging from 7.0 to 1.7 mg/g.[165]

Typically, cationic surfactants are quaternary ammonium compounds (QAC), with the positive charge on the N atom. Nonetheless, cationic surfactants are more expensive than anionic surfactants.[5] Zwitterionic surfactant contains both anionic and cationic surface charges, such as carboxyl and sulfonate betaines.[166] Nonionic surfactant bears no apparent

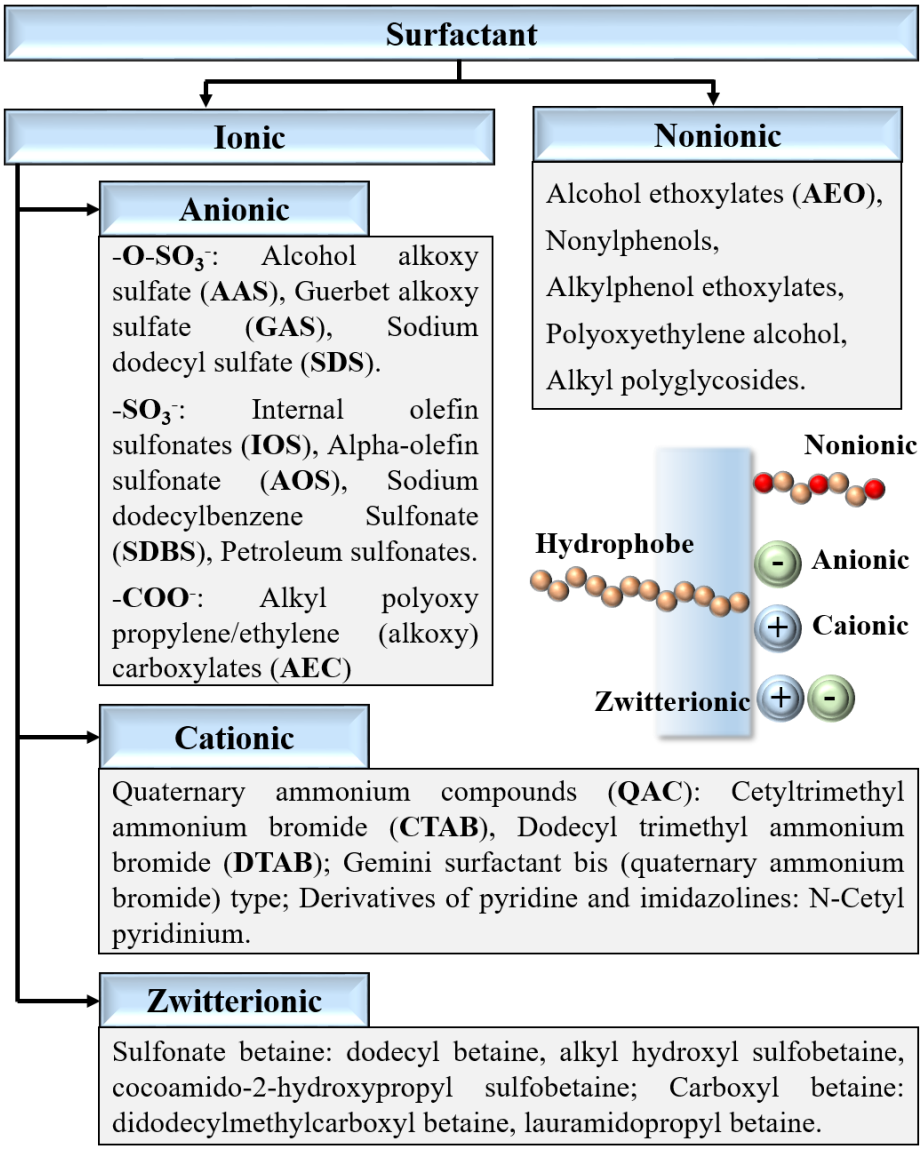

Figure 3. Surfactant types and classification according to their chemical structures.[5,11,16,40,167]

ionic charge, consisting of non-dissociable functional groups such as alcohols, phenols, ethers, esters, or amides.[5] When opposite charges are present among surfactant and rock surface, surfactant adsorption tends to be higher. Generally, adsorption of anionic surfactants is lower in sandstone rocks, whose surfaces are negatively charged. Whereas, the adsorption of cationic surfactant is higher on sandstone rocks compared with anionic surfactants. On positively charged carbonate surfaces, the adsorption of cationic surfactants is less but has a higher adsorption for anionic surfactants. Similar behavior is also observed for amphoteric surfactants, which have a greater adsorption on kaolinite surface than anionic surfactant

because of the strong electrostatic interactions.[168] The nonionic surfactants adsorption on clay minerals was found to be much higher than anionic surfactants.[68]

In a commercial surfactant system, it generally contains surfactant mixtures with a variety of hydrophobic and polar groups. Interactions among surfactant mixtures can result in remarkable interfacial effects owing to changes in surfactant adsorption and also in the charge density of rock surfaces.[37] In terms of anionic-nonionic surfactant blends, the presence of nonionic surfactant decreased adsorption of anionic surfactant on positively charged surfaces, but the adsorption of nonionic surfactant was enhanced.[169] Similarly, the amounts of both nonionic surfactant adsorbed on shale or sandstone surfaces were reduced in the presence of anionic surfactant.[170] On the other hand, the amount of either anionic surfactant or nonionic surfactant adsorption can be minimized on clay minerals when they were mixed with each other.[171] Results showed that the synergistic effect for the coadsorption of cationic-nonionic surfactant mixtures induced wettability alteration of rock surfaces.[172–174] The underlying mechanism for the adsorption of cationic-nonionic surfactant mixture was thought to be more or less the same for the anionic-nonionic surfactant mixture: hydrophobic interactions and the reduction of the electrostatic repulsions. Because of the risk of precipitation or formulation instability, the adsorption behavior of cationic-anionic surfactant mixtures was seldomly investigated, and more focus was put on their micellar and interfacial properties.[175,176]

The added chemical groups greatly affect surfactant adsorption, such as propoxy (PO, C_3H_6O) and ethylene oxide (EO, C_2H_4O) groups. It was found that surfactant adsorption on kaolinite clay declined with the increase of the number of PO groups.[177] This is because increasing PO groups make surfactants more hydrophobic and the stronger hydrophobic interactions relatively lessen the interactions between polar heads of the surfactants and the specific sites on the kaolinite clay surfaces. Increasing the EO to hydrocarbon ratio resulted in a substantial

decrease in the adsorption of poly(ethylene glycol) monoalkyl ethers on silicas.[178] A lower adsorption was observed on calcite for ethoxylated alkyl aryl sulfonate surfactant compared to its non EO counterpart.[162] Moreover, by incorporating EO units into the surfactant molecule, high solubilization of oil and brine phases were achieved due to the hydrogen bonding of EO and water.[179] Unlike SDS and SDBS systems, the EO groups may bind Ca^{2+} and the interaction between Ca^{2+} and $–O\text{-}SO_3^-$ group decreases, consequently, the anionic surfactant would not easily precipitate by Ca^{2+}, *i.e.*, the Ca^{2+} tolerance of anionic surfactants is improved by the introduction of EO groups.[180] A nonyl phenol with 5.1 EO groups has the same hydrophilicity as a dodecylphenol with 8.3 EO groups, but the second one produces twice as much solubilization of octaneand water, whose hydrophilicity can be varied continuously by changing the average EO groups.[181] It was also observed that more the number of EO groups in the anionic surfactant, the higher was the aqueous stability at higher salinities.[182] The influence of the number of EO and PO groups on phase behavior of Guerbet alcohol sulfates have been investigated to select optimal surfactant structures for cosurfactant-free microemulston systems .[183] Moreover, compared to its linear counterpart, the branched structure of phosphate ester surfactants is beneficial to improve the adsorption performance of the gas-liquid interface, but not to the adsorption of the solid-liquid interface.[184] The position of the branching of sulfonate group has a measurable effect on the surfactant adsorption on the alumina surface.[185] Increasing percent of PO and increasing degree of hydrophobe branching of the surfactants leads to increase surfactant adsorption.[186]

Surfactant concentration is the most crucial factor to determine the adsorption of the surfactant and adsorption isotherms (Section 2.2). At low surfactant concentration below the CMC, surfactant adsorbs as monomers on the mineral surfaces. The adsorption is due to electrostatic interactions for ionic surfactants and hydrogen bonding for nonionic surfactants.[36] As surfactant concentration increases, lateral (hydrophobic) interactions are

significant for later surfactant adsorption and surface aggregation takes place. When reaching the CMC, adsorption achieves a plateau and further increasing surfactant concentration gives no influence on adsorption. It has been accepted that surfactant concentration in chemical slugs should be substantially above its CMC so that micellization can be initiated. At low surfactant concentrations but above the CMC, the volume of the middle-phase microemulsion (Winsor III) is minute and its presence may not be visually detected. On the other hand, at high surfactant concentrations, more of the excess oil and water phases are solubilized and form the Winsor III which give rise to a higher recovery.[41] However, too high surfactant concentration may cause the building of undesirable pressure gradients by the end effect, against the direction of flow.[187]

3.2 Solution chemistry

The adsorption of surfactants is strongly influenced by the chemical properties of the solution such as pH, salinity, and ionic composition. A mineral surface can be positively or negatively charged by the dissociation behavior of surface groups or by the adsorption of ions from the aqueous solution, which is pH dependent. Anionic surfactants tend to adsorb on positively charged surfaces, whereas cationic surfactants are attracted to negatively charged ones. Around neutral pH, silica surface is primarily negative charged, while carbonate surface is positively charged.[11,75] Adjusting the solution pH, it will influence rock surface charges, and therefore alter the adsorbed surfactants. When solution pH was increased to 11, the adsorption of anionic surfactants was largely reduced on silica surfaces.[81] It is reported that anionic surfactants have been extensively used in sandstone reservoirs because of the fact of less adsorption compared with nonionic, cationic and zwitterionic surfactants.[188] The adsorption of anionic surfactants on Indiana limestone revealed two adsorption mechanisms taking place: charge regulation by electrostatic attraction at lower pH values, and adsorption via hydrogen bonding at higher pH values.[189] In the presence of Ca^{2+} ions, the adsorption of

anionic alcohol alkoxy sulfate (AAS) surfactant increased with increasing pH (**Figure 4a**), while a different behavior was observed for Na^+ ion that AAS adsorption decreased with an increase of pH and there was negligible AAS adsorption with Na^+ above pH 8.[53] In the absence of salt, the amount of a cationic surfactant adsorbed on silica increased with the increasing solution pH due to electrostatic attractions.[190]

The ionic composition of the surfactant flooding solution is another significant factor influencing the surfactant adsorption to rock surfaces. Divalent cations, such as Ca^{2+}, are capable of acting as ionic bridges between anionic surfactants and negatively charged surfaces, and therefore favoring anionic surfactant adsorption.[53,54,91,191,192] The rate and quantity of anionic surfactant adsorption can be governed by the introduction of Ca^{2+}.[193] On silica surfaces, it was shown that the amount of adsorbed SDS surfactant doubled when the present sodium ions were substituted by calcium ions.[194] In **Figure 4b** and **c**, it was observed that the adsorbed AAS had a maximum at the Ca^{2+} concentration of ~200 mM, whereas the change of $CaCl_2$ by NaCl showed negligible AAS adsorption.[53] The higher the concentration of Ca^{2+}, the more cation bridges are formed (**Figure 4d** and **e**). Based on the Voigt-Kelvin model, multilayer adsorption of surfactants is calculated as many as 4-6 monolayers. Applying the mixed cation (Ca^{2+} and Na^+) solutions, the adsorbed AAS increased linearly with increasing fractions of Ca^{2+} and it was estimated that Na^+ could compete with maximal ~30% adsorption sites on clay.[53] A different situation was found on the calcite surface and Na^+ was considered as an indifferent ion for the surfactant adsorption, while the increase of the Ca^{2+} concentration did show an increase in AAS surfactant adsorption.[54] The increasing ionic strength with NaCl yielded a more rigid adsorbed layer of cationic behenyl trimethyl ammonium chloride (BTAC, C22) on the silica.[195] In $CaCl_2$ solution, the adsorbed BTAC film became soft and highly dissipated at pH 5.7, while it was less soft at pH 10. These

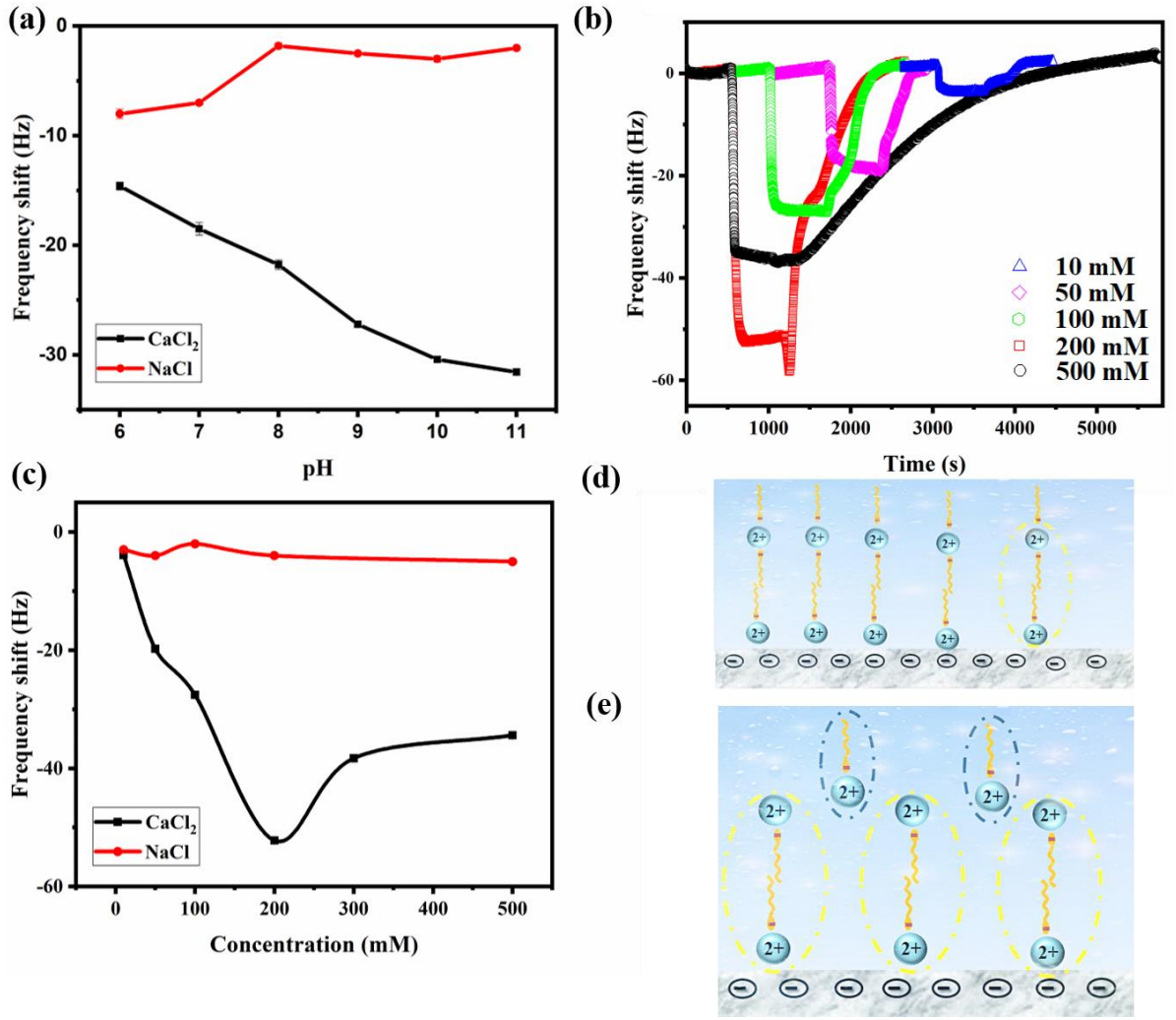

Figure 4. (a) Effect of pH on the surfactant adsorption to the clay surface. (b) Real-time observed frequency shifts upon addition of 0.15 wt % AAS and subsequent flush without AAS at pH = 9 and room temperature with varying $CaCl_2$ concentrations. (c) Observed maximum frequency shifts as a function of NaCl and $CaCl_2$ concentration. (d) Schematic illustration of the adsorbed AAS surfactants to the clay surface via Ca^{2+} bridging for the multilayer adsorption, such as the double layer film in the black circle. (e) Screening effect of Ca^{2+} leads to the formation of positively charged $Ca(RSO_4)^+$ complexes (red dash circle). Reprinted and reproduced from.[53]

rigidity inconsistencies were likely because of the strong sorption of $Ca(OH)^+$ at higher pH. For polyoxyethylenic nonionic surfactants, three different adsorption behaviors (increase, decrease, and no alteration) had been found in the presence of NaCl, which was due to the interactions of salt cations with various surface hydroxyl groups and surface impurities.[196] Only one behavior (a rise in adsorbed amounts) was observed for the adsorption of anionic oxyethylenic surfactants on quartz and kaolin surfaces when NaCl was added.[196] However, anionic surfactants can severely precipitate in high Ca^{2+} concentration solution.[197]

It is generally observed that an increase of the solution salinity contributes to the adsorption of surfactants, which is ascribed to the decrease in the Debye screening length, thus lowering the electrostatic repulsions between surfactants and mineral surfaces.[15,191] Salinity can also change the solubility, surface activity, aggregation property of nonionic surfactants, and therefore it may exert an influence on the surfactant adsorption.[72] Furthermore, salinity alters the surface charge of mineral surfaces, thereby influences surfactant adsorption. AlQuraishi et al.[198] had reported a considerable increase in the negative surface charges of sandstone rock when high salinity seawater was switched to diluted low salinity (LS) seawater. As a result, the adsorption of anionic surfactant was reduced in LS solution because of the increased number of negatively charged sites.[199] A cEOR process combining the injection of LS and surfactant has been proven to be more effective in comparison with only LS or only surfactant flooding.[200,201] The decrease in surfactant adsorption from high salinity to LS primarily relied on the reduced amounts of divalent cations and the electric double layer effect played a minor role[53]

3.3 Rock mineralogy

A sandstone rock comprises large amounts of quartz (silica, SiO_2), and minor fractions of carbonate, clay and silicate minerals.[188] Except quartz, typical Berea sandstone consists of an average of 5 to 9 wt% clay minerals (mainly kaolinite and illite).[202] Most of cEOR applications have been carried out in sandstone reservoirs, which are homogeneous.[2] Anionic surfactants are usually preferentially employed in sandstone reservoirs because the electrostatic repulsions between the anionic surfactant and sandstone reservoir surface inhibits the adsorption.[203] At higher pH, silica exhibits negligible adsorption of anionic surfactants.[41] On silica, alumina, and gibbsite surfaces, different adsorption mechanisms of sodium hexanoate was proposed by the presence of Ca^{2+}.[204] Wang et al. concluded that surfactant adsorption on Loudon and Berea sandstones (Payette County, IL) resulted

primarily from the presence of clays.[205] The presence of clay minerals is important for the adsorption of surfactant because of the heterogeneous surface charge.[206] The adsorption of the nonionic poly(vinylpyrrolidone) (PVP) and the anionic SDBS mixtures on kaolinite surface is governed by the surface charges.[207] To understand LS water flooding mechanisms, both clays and divalent cations were essential, especially for the surface reaction.[42,208] The calcium-surfactant complexes had a significant role in the adsorption on kaolinite.[209] The cation-dependent anionic surfactant adsorption on clay minerals was investigated in detail with varying concentrations of the monovalent Na^+ and divalent Ca^{2+}.[53] Adsorption capacities of nonionic surfactant (Triton X-100) depended on the mineral content of the rock in the order of illite >feldspar >montmorillonite >kaolinite.[210] In this context, more focus of surfactant adsorption can be put on different clay types, structures, composition distributions, and content over the surface.

Carbonate reservoirs, approximately taking 60% of the world's oil reservoirs, are composed primarily of salt-like carbonate minerals.[211] The two major types are limestone, which is predominately calcite or aragonite (less stable crystal form of $CaCO_3$), and dolomite ($CaMg(CO_3)_2$), together with impurities, such as $CaSO_4$, $CaSO_4 \cdot 2H_2O$, and magnesite ($MgCO_3$). It was reported that less than 20% of cEOR projects were implemented in carbonate reservoirs because of the challenges in the complexity of carbonate compositions and surface properties, matrix pore structures, fracture densities, aperture and orientations, as well as oil types.[70] The main issue with ASP flooding is the precipitation caused by the reaction of injected alkalis and surfactants with divalent cations from the dissolution of carbonates.[212] This also makes the investigation of adsorption on carbonate rocks much more complex compared to sandstone surfaces. Static adsorption experiments revealed that cationic surfactants may exhibit significantly less adsorption on carbonate minerals than anionic surfactants.[213] However, if abundant clay and silica exist in the carbonated formations, a

significant adsorption of cationic surfactants can be found.[214] Ma et al. pointed out a slight adsorption of a cationic surfactant on the synthetic calcite without silica or clay, but the quantity of adsorbed surfactant was higher on natural limestone.[188] Through electrostatic attractions and hydrogen bonding, cationic dodecylamine adsorbed on CO_3^{2-} sites of calcite surface, which induced a moderate zeta potential increase for calcite.[215] Also, the duration required to reach adsorption equilibrium was much longer onto Berea sandstone than either Indiana limestone or Lockport dolomite because of its multicomponents and complex porous structures.[216]

There are also a few investigations on unconventional shale reservoirs, which are comprised of various minerals of calcite, dolomite, clay, quartz, kerogen, etc. A Langmuir isotherm was fitted to adsorption of a nonionic surfactant on a preserved reservoir shale, which plateaued at 5 mg/g of adsorption at concentrations greater than the surfactant CMC.[217] Zhang et al. observed a low adsorption capacity of the blended surfactant (0.62 mg/g) on the Bakken formation (consists of Lower Shale Member, Middle Dolostone/ Siltstone Member, and Upper Shale Member.), which was still higher than 0.1 mg/g in comparison with the conventional permeable rocks.[218] The adsorption capacity of shale heavily depended on the types of surfactants and mineral compositions. The cationic CTAB surfactant displayed the highest adsorption capacity in mass units on an Eagle Ford reservoir shale, followed by nonionic nonyl phenol ethoxylate and then anionic IOS surfactant.[165] These adsorptions can be dominated by the content of calcite and clay in the shales.[165] Dynamic adsorption measurements on siliceous and carbonate Bakken shales showed a higher adsorption of negatively charged surfactants to carbonate rocks and more positively charged surfactants adsorbed on siliceous surfaces.[219]

3.4 Temperature

Surfactant adsorption is generally an exothermic process ($\Delta H^{\circ} < 0$), which could be either enthalpy driven or entropy driven.[11,15,36] In regard to surfactants with low adsorption density, the adsorption density increases with increasing temperature (enthalpy driven adsorption). However, the reverse happens for surfactants with high adsorption density, and the adsorption density decreases with an increase of temperature (entropy driven adsorption).[11] At high temperature, the relatively high kinetic energy contributes to destabilize aggregated organizations, resulting in the low surfactant adsorption. This adsorption behavior was observed by Azam et al.,[199] who investigated the anionic surfactant adsorption onto Berea sandstone. A reduction of the SDS adsorption on hydrotalcite-like minerals (anionic clay) was also found at high temperature.[220] In the absence and presence of salts, the adsorption capacity of SDS on kaolinites decreased with increasing temperature.[221] Liu et al. uncovered an interesting observation that increasing the temperature from 23 to 65 °C showed first a small increase in anionic AAS surfactant adsorption, succeeded by a reduction of approximately 20%.[53] They found that the CMC would increase at higher temperatures and the increased free surfactant monomers led to the small increasing adsorption, while later adsorption process was entropy driven.[53] Effect of temperature on the CMC of surfactant systems is determined by various factors including surfactant chain lengths and head groups, ionic strengths, etc.,[222] and this effect is greater for anionic surfactants.[223] In addition, the increase in temperature decreased the viscosity of the surfactant solution.[12,199] It would affect the surfactant diffusivity and restricts the movement of surfactant molecules to the rock surface.[221]

The adsorption of nonionic surfactant generally increases with increasing temperature. Corkill et al. proposed the solvation effect for the high adsorption.[224] The increase in temperature progressively dehydrates the head groups of surfactants, rendering it to be less hydrophilic and more compact, and therefore increases the surface activities and adsorption

amounts. This behavior also depends on the surfactant concentrations. At low concentrations, adsorption of the nonionic surfactant onto crushed Berea sandstone decreased with an increase in temperature, whereas the opposite was found in high concentrations.[225] The phase separation (cloud point) of nonionic surfactant at high temperature could likely result in the decrease of surfactant concentration.[41,226] At high temperature conditions of 95 °C, the zwitterionic surfactant was designed in extremely low CMC values to lower adsorption by reducing free monomers of surfactant in solution.[227] With 90-110 °C, it was found that adsorption of zwitterionic surfactants on oil sands was higher than on clean sands, which can be attributed to hydrogen bonding interactions.[228] However, zwitterionic surfactants are more expensive compared with other surfactants. Most of the surfactants will generate either degradation or precipitation at temperatures above 120 °C.[223] Reservoirs with high temperatures up to 120 °C are still suitable with surfactant flooding.[229] Meanwhile, the effect of temperature on the phase behavior of surfactant-oil-water mixtures, wettability, IFT, imbibition rates, and viscosity of oil should also be considered in cEOR. At reservoir conditions, the high temperature is usually accompanied with high pressure. Increase in pressure caused a reduced surfactant solubility,[230,231] but the effect on surfactant adsorption is not clear.

4. Reducing surfactant adsorption

How to mitigate surfactant adsorption is one of the main issue for a cost-effective surfactant flooding in cEOR. Recent applications of adsorption inhibitors or sacrificial agents, and chemical formulations to reduce surfactant adsorption have been discussed.

4.1 Alkalis

In general, the use of alkalis is to mitigate adsorption of surfactants on the rock surfaces by increasing the solution pH and sequestering divalent ions.[36,80] This has been extensively applied in sandstone reservoirs as alkali forms a negatively charged surfaces that result in a

strong electrostatic repulsive force to inhibit anionic surfactant adsorption.[164] Alkali injection also generates sodium naphthenate (soap) in situ from its reactions with naphthenic acids of crude oil.[2] Although generating soap is important in itself, synergies between the in situ soaps and the injected surfactants is probably even more important. The used alkalis include strong alkali sodium hydroxide (NaOH, caustic soda), weak alkali sodium carbonate (Na_2CO_3, soda ash), sodium bicarbonate ($NaHCO_3$), sodium metaborate ($NaBO_2$), sodium orthosilicate (Na_4SiO_4), sodium phosphate (Na_3PO_4), ammonium hydroxide (NH_4OH), and organic alkalis.[18,164,232–235] Na_2CO_3 is the most commonly used alkali because it possesses an attractive combination of cost, buffered alkalinity, and control of calcium cations. It was observed that Na_2CO_3 as an alkali reversed the surface charge of calcite from positive to negative, leading to lower adsorption of anionic surfactants that was not observed with NaOH.[236] The possible reason was that the hydroxide was not a potential determining ion for carbonate surfaces whereas carbonate ion was. Especially at low salinities, the use of Na_2CO_3 was found to substantially decrease the adsorption of anionic surfactants on the carbonate surface.[237] Na_2CO_3 is preferred for sandstone applications instead of NaOH because of the high levels of silica dissolution resulting in silicate scale and wellbore erosion for NaOH and the low average loss rate of alkali and surfactant for Na_2CO_3.[233,238,239] However, recent studies on Indiana limestone suggested the use of NaOH to lower the surfactant retention.[240–242] The reasons for NaOH selection were the higher pH of NaOH compared with Na_2CO_3 or ammonia, suppressing and slowing down the dissolution of calcite, and less alkali consumption by calcite, dolomite, and quartz. In the meantime, $NaHCO_3$ is a good choice for reservoirs containing clay minerals.[5] In carbonate reservoirs where $CaSO_4$ or $CaSO_4 \cdot 2H_2O$ widely exists, the addition of Na_2CO_3 or NaOH leads to the precipitations of $CaCO_3$ or $Ca(OH)_2$ in hard saline.

To alleviate the corrosion and scale issues associated with Na_2CO_3 and NaOH, other weaker and organic alkalis were proposed. At low ammonia concentration, static adsorption tests showed low surfactant adsorption at pH >9 and it did not precipitate calcium from solution.[164] Ammonia is logistically preferred because of its low molar mass and the possibility for delivery in offshore and remote environments. As an alternative alkali, $NaBO_2$ could offer very low retention of surfactant, and tolerate as high as 6000 ppm Ca^{2+} and Mg^{2+}.[243,244] Sodium tetraborate ($Na_2B_4O_7$) was also suggested that had the advantage of high salinity tolerance and better performance on reducing surfactant adsorption onto the kaolinite in comparison to the conventional Na_2CO_3 alkalis.[168] Recently, organic alkalis have gained much attention due to the non-toxicity and biodegradability, including organic amines, organic phosphates, etc., and their aqueous solutions are alkaline. Berger and Lee firstly evaluated the effect of replacing inorganic alkalis with organic alkalis, and found high salinity and high divalent cation tolerances of organic alkalis.[245] Whether saline water was softened or not had no significant impact on the performance of the organic alkali. Adding organic alkali helped to reduce amphoteric surfactant adsorption in core flood experiment.[227] Organic alkali ethanolamine (EA) reduced adsorption of surfactants and minimized formation damage because of low EA consumptions at high temperature.[246] Other aspects of compatibility with formation and injection water, IFT reduction, wettability alteration, emulsification, viscosity, formation damage, recovery potential of organic alkalis have been also extensively discussed,[16] but until now, no field test using organic alkali is reported.

4.2 Polymers

Polymers are habitually used as co-injectants with surfactants to improve the viscosity of solutions, and therefore increase the mobility ratio and volumetric sweep efficiency of the reservoir.[7,14] Although the interactions of surfactant and polymer in solution have been widely investigated, their interactions at rock surfaces and the effects on adsorption are less

studied. To mitigate anionic surfactant adsorption to reservoir rocks, addition of anionic polyelectrolytes as the sacrificial agent can be very useful, because they compete with anionic surfactants for the binding sites on rock surface (**Figure 5a and b**). Since the final loss of such sacrificial agents is less expensive compared to surfactants, the use can be cost effective. In the early studies, lignosulfonate, a cost-effective modified waste byproduct from the paper industry, carried anionic charges in solution and had been studied to reduce surfactant adsorption. Hong et al. reported lignosulfonate as an inexpensive preflush chemical to lower the petroleum sulfonate adsorption by more than 50 wt% in Berea cores.[247] Tsau et al. revealed that lignosulfonate decreased the adsorption of the primary surfactant Chaser™ CD1045 by 24-60 wt% in Berea sandstone and 15-29 wt% in Indiana limestone core samples.[248] Also sodium polyacrylate (PA) of MW larger than 4500 g/Mol was able to significantly reduce anionic surfactant adsorption on both Berea sandstone and Carlpool dolomite rocks (Kocurek Industries and Earthsafe Organics Carlpool Products).[79,249] The molar ratio of PA to $CaSO_4$ was an essential variable governing the competitive adsorptions between anionic surfactant and PA.[250] A different relationship between polymer MW and surfactant adsorption was found for poly(ethylene oxide). Increasing the MW of poly(ethylene oxide) resulted in a decrease of cationic surfactant adsorption on silica.[251] At totally dissolved solids (TDS) of over 300,000 mg/l, after the addition of polystyrene sulfonate (PSS), the surfactant adsorption was significantly reduced by more than half.[252] Experiments carried out by Weston et al. also demonstrated that adding PSS polyelectrolyte on positively charged metal oxide, alumina, and the cationic polyelectrolyte polydiallyl dimethylammonium chloride, on negatively charged metal oxide and silica, decreased the adsorption of anionic and cationic surfactants, respectively.[253] When carbonate cores were preflushed with sulfonated polyacrylamide (SPAM) polymer and then followed by injection of both surfactant and SPAM, or co-injected with surfactant and SPAM, an average reduction

of surfactant adsorption was around 50 wt%.[254] Others have shown that the injection order of polymer addition has a strong effect on the surfactant adsorption and the preflush method seems to be more effective.[253,255,256] With lignin preflush batch method, significant decrease in adsorption of 4-octylphenol polyethoxylated (TX-100) and SDS on illite and kaolinite were 53.2 and 50 wt%, respectively.[257] The use of polyelectrolytes has also been evaluated onto high surface area shales (mainly calcite, dolomite, quartz, and illite)[258] and the specific counterions (bromide, chloride, *etc.*) made great influence on the co-adsorption of polyelectrolyte and surfactant onto silica surfaces.[259]

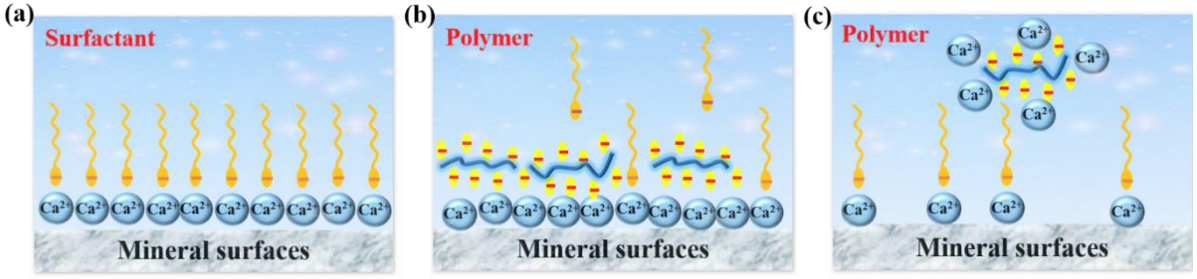

Figure 5. (a) Schematic illustration of the adsorption of anionic surfactant on mineral surfaces through cation bridging. (b) Polymer polyelectrolytes as the sacrificial agent compete with anionic surfactants for the rock surface binding sites, reducing the adsorption of anionic surfactant. (c) polymers as chelating agents increase the negative potential on the rock surfaces, and hence the surfactant adsorption is reduced.

Another method is to add chelating agents (**Figure 5c**), such as, ethylenediaminetetraacetic acid (EDTA), aminopolycarboxylic acid (APCA), diethylenetriaminepentaacetic acid (DTPA), and polyphosphates, which can chelate divalent cations and increase the negative potential on the rock surfaces, and therefore the surfactant adsorption is reduced.[260–262] In a calcium brine environment, the addition of polyphosphates to both preflush and micellar slugs significantly reduced surfactant loss, but its effectiveness was somewhat poor in a sodium brine environment.[261] EDTA or sodium citrate is effective to remove a small amount of trivalent Fe and Al, leading to much lower adsorption on an oxidized, iron-containing outcrop.[263] Moreover, the chelating agents can delay and inhibit scale formation, and complex with the salt-forming cations and prevents their interactions with surfactants.[264]

4.3 Nanoparticles

Addition of NPs to the surfactant solution is beneficial to keep surfactant molecules in the bulk solution. One approach to reduce surfactant adsorption is to decrease the adsorption area onto rock surfaces using NPs. As a result, the contact probability between surfactants and rock surface is reduced and there will be more surfactants in bulk solution. Static and dynamic adsorption experiments (**Figure 6a and b**) revealed that adding hydrophilic silica NP (SNP) reduced the surfactant adsorption on rock in deionized water and the optimal SNP concentration was considered to be 0.2~0.3 wt%.[265] Under the conditions of 80 °C and artificial seawater as injection brine, pre-treatment of the sandpack with SNPs reduced surfactant adsorption by a factor of three.[266] Surface tension trends of different concentration of SDS in absence and presence of 1 wt% SNP and Al_2O_3 NPs before and after equilibration with kaolinite revealed that SDS adsorption reduced by 38% in the presence of Al_2O_3 NPs and 75% in the presence of SNPs.[267] A higher adsorption reduction capacity of SNPs than Al_2O_3 NPs was also found for soap-nut surfactant, which can be attributed to almost round structures of SNPs as compared with Al_2O_3 NPs having sharp edges.[98] In another study, Zargartalebi et al. reported a general reduction in surfactant adsorption due to the presence of SNPs, and this reduction was higher for hydrophobic SNPs than hydrophilic SNPs.[268]

Another approach is to adsorb surfactants onto NP surfaces (**Figure 6c**). Ahmadi and Shadizadeh suggested that hydrophobic interactions between hydrophobic groups of SNPs and hydrophobic tails of surfactants resulted in more surfactant adsorption onto hydrophobic SNP surfaces and less adsorption to the kaolinite surface, compared to hydrophilic SNPs.[269] Zhong et al. proposed the competitive adsorption of surfactant on SNPs and rock surfaces. When SNPs were present, there would be less nonionic surfactant adsorption, and SNPs with a smaller size and stronger surfactant carrying capacity had shown a higher efficiency.[270] A ligand functionalized SNP effectively reduced zwitterionic surfactant adsorption loss and

made the oil-wet solid surface toward a more water-wet condition beneficial for water imbibition and oil displacement.[271] The adsorbed amount of cationic, anionic, and nonionic surfactants onto SNPs decreased in the order CTAB > nonionic polyoxyethylenesorbitan monolaurate (Tween 20) > SDS and its adsorption decreased as temperature increased.[272] To obtain more surfactant adsorption onto NP surface, Betancur et al. synthesized magnetic iron core-carbon shell NPs. The core flooding tests demonstrated that this novel NPs reduced 33% the adsorption of surfactant mixtures and the NP-surfactant flooding obtained an oil recovery up to 98%.[273]

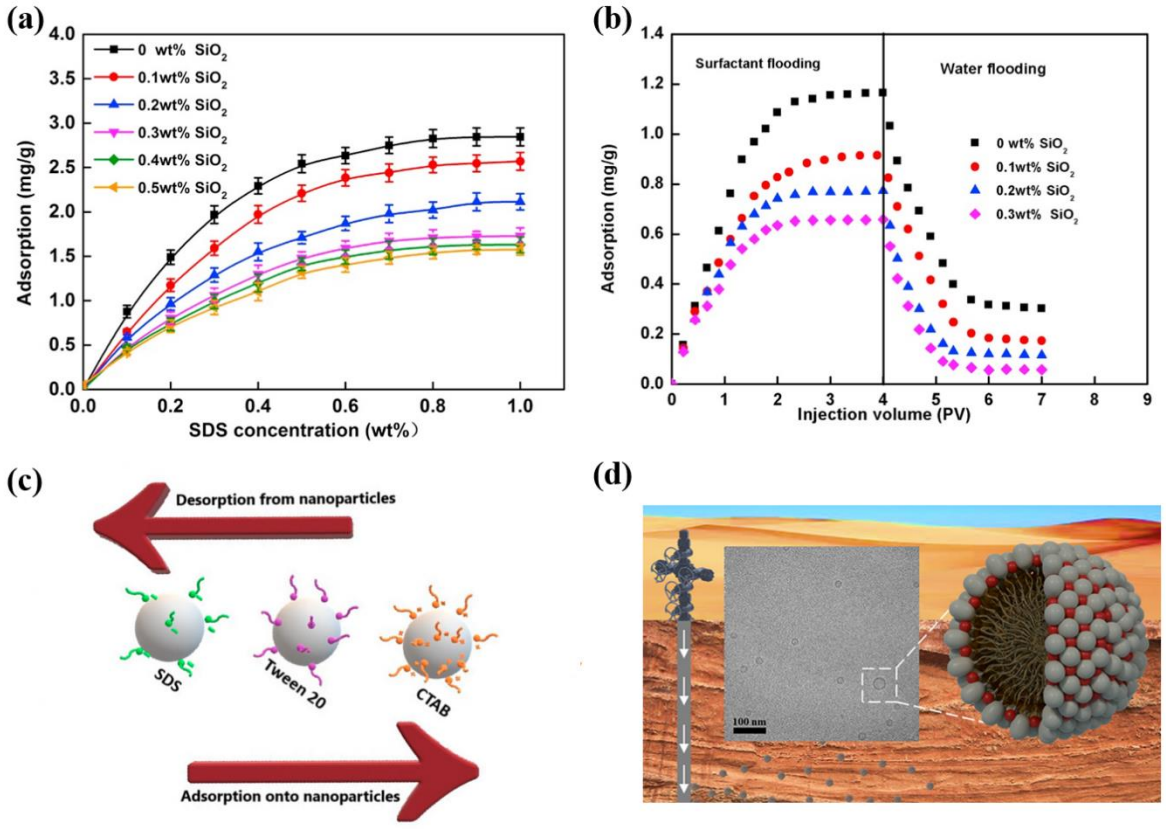

Figure 6. The effect of SNP on static adsorption (a) and dynamic adsorption (b) of SDS. Adapted with permission.[265] (c) Interactions between SNP and various surfactants. Adapted with permission.[272] (d) NP delivery for efficient surfactant applications in harsh conditions. Adapted with permission.[274]

Borrowing the concept of the targeted delivery combined with controlled drug release,[275] NPs can be also used to deliver surfactant inside a porous media (**Figure 6d**). There are two main functions of NPs: (1) reduce surfactant adsorption on the rock surface, and (2) form a synergy effect with surfactant, such as IFT reduction, oil recovery increase. Avila et al. used cross-

linked polystyrene NPs as surfactant carriers. These NPs swelled when in contact with the oil phase, and surfactants were released, reducing oil-water IFT.[276] Because of a synergistic effect between NPs and surfactant action at the oil-water interface, partially sulfonated polystyrene NPs inhibited surfactant adsorption and induced an increase of oil recovery of up to about 13%.[277] Using carbonaceous NPs (multi-walled carbon nanotubes and carbon blacks) as surfactant carriers, competitive adsorption of anionic surfactant on NPs surface against sand was beneficial to decrease the surfactant losses.[278] By using TiO_2 NPs carriers, surfactant adsorption can be substantially reduced, *i.e.* half of the initial adsorption value.[279] Organic NPs carriers were also achieved with lipid beeswax and nonylphenol ethoxylate (NPE10) surfactant, showing a storage capacity of 96% of surfactants and high mobility in porous structures of unconsolidated sandpack column.[280] Moreover, a surfactant carrier system based on the complexation of surfactant/beta-cyclodextrin (β-CD) was developed and QCM-D measurements confirmed a 50% reduction of surfactant adsorption in complex-state compared to the adsorption of surfactants in free-state.[281] Cortés et al. reported null surfactant adsorption to rock surfaces with nanocapsules. Displacements tests showed that nanocapsules could increase the oil recovery with lower pore volumes injection (43% less) than when using a dissolved surfactant.[282] Later, petroleum sulfonate nanocapsules produced a highly stable nanofluid at elevated salinity (~56,000 mg/L) and temperature (~100 °C), reduced crude oil-high-salinity water IFT by 3 orders of magnitude (from ~10 to 0.008 mN/m), and enhanced mobilizations of the trapped crude oil from the carbonate rocks. Under simulated reservoir conditions, the relatively low levels of irreversible nanocapsules adsorption was roughly 0.62 mg/g of the rock, which was lower than that of most economic conventional EOR surfactant.[274] Nourafkan et al. developed an innovative concept of using nanodroplet as a surfactant carrier and it promoted higher oil recovery rate around ~8%, while reducing the

surfactant adsorption nearly 50% on sandstone rock surface compared with the micelle forms of surfactants.[283]

4.4 Co-solvents and ionic liquids

To optimize high performance surfactant formulations, co-solvents are often added to obtain better phase behavior, lower microemulsion viscosity, and improved surfactant-polymer compatibility.[284–287] ASP coreflood experiments with iso-butanol (IBA) alkoxylates and phenol alkoxylates co-solvents revealed negligible phase trapping and extremely low levels of surfactant retention (varied from 0.02 to 0.1 mg/g rock).[284] Low retention means low adsorption and more surfactants can be used to recover oil from the reservoir. Novel cosolvents and surfactants with ultrashort hydrophobes (PO groups) had been developed to show excellent performance with very low cosolvent and surfactant retention in cores.[285] Dwarakanath et al. used co-solvents to optimize surfactant behavior, alleviate microemulsion phase trapping, and decrease surfactant retention in conditions where the optimal salinity was considerably higher than reservoir salinity.[286] Arachchilage et al. optimized surfactants with co-solvents formulation to have a retention of <0.1 mg/g of surfactant, which significantly reduced chemical cost.[287] Sahni et al. applied a tiny amount of alcohol ethoxylate as co-solvent or co-surfactant to make the ASP slug clear, leading to a higher oil recovery and lower surfactant retention.[288]

Within the last few years, ionic liquids (ILs) have been proposed as EOR chemicals to show its applications in wettability alteration, IFT reduction, high oil recovery rate, and shale inhibitors.[5,289,290] More recently, Hanamertani et al. firstly introduced ILs as sacrificial agents to reduce surfactant adsorption.[291] The potential of ILs for inhibiting surfactant access to the rock surface, resulting in the reduction, highly depended on types of used ILs and surfactants. It was observed that the addition of imidazolium-based and eutectic-based (deep eutectic solvent, DES) ILs can be used to decrease IOS adsorption by three times, whereas DES also

greatly reduced in-house surfactant having a much longer and complex hydrocarbon chain adsorption compared to other ILs.[291] Apart from these advantageous properties of ILs, they are cost-efficient and commercially available.

4.5 Salinity gradient

In surfactant flooding, a negative salinity gradient was proposed to mitigate surfactant adsorption and phase trapping, and keep surfactant in the Winsor Type III phase environment for as long as possible during the flooding process.[292] The negative salinity gradient means salinities of preflush water slug, surfactant slug, and post-flush slug (water or polymer drive) in descending order (**Figure 7**). The high salinity formation brine is firstly replaced by the surfactant formulation at a salinity close to the optimal salinity (Winsor III phase microemulsion with ultra-low IFT, but high surfactant retention), and then, displaced by a water or polymer drive formulated at a lower salinity (Winsor I phase microemulsion with low surfactant adsorption).[80,293] Because of surfactant adsorption and retention, the surfactant concentration will be decreased as the surfactant solution moves forwards and the optimum salinity decreases with surfactant concentration.[21] Thus, the decreasing salinity is consistent with the decreasing optimum salinity so that the optimum salinity is maintained when the surfactant solution move forwards.[294] The ultimate adsorbed chemicals would be significantly lower compared to a constant salinity injection scheme, while maintaining higher oil recovery efficiency.[295] When a salinity gradient was considered, the surfactant adsorption level was less than a factor 3 of the reference adsorption without salinity gradient.[296] A new model was developed to comprehensively evaluate the role of a salinity gradient on recovery profile, and the negative salinity gradient was found to provide a better recovery factor compared to the non-negative salinity gradient injection strategy.[297] The associated problems with this injection strategy (salinity gradient) can be the possibility of inappropriate mixing of brines, availability of soft brines like in off-shore conditions, technical and logistic issues.[80,298]

Tabary et al demonstrated that efficiency of a salinity gradient design substantially decreased when hard brines were considered.[299] Moreover, the effect of salinity gradient was typically less efficient on carbonate rocks than sandstone rocks because the adsorption isotherm shape on calcite rock exhibits a highly different shape as impact of salinity on sandstone is significantly lower.[293] As for a salinity gradient, a compromise has to be made between the main slug and post-flush slug conditions to guarantee optimal performances of adsorption tests and oil recovery experiments.

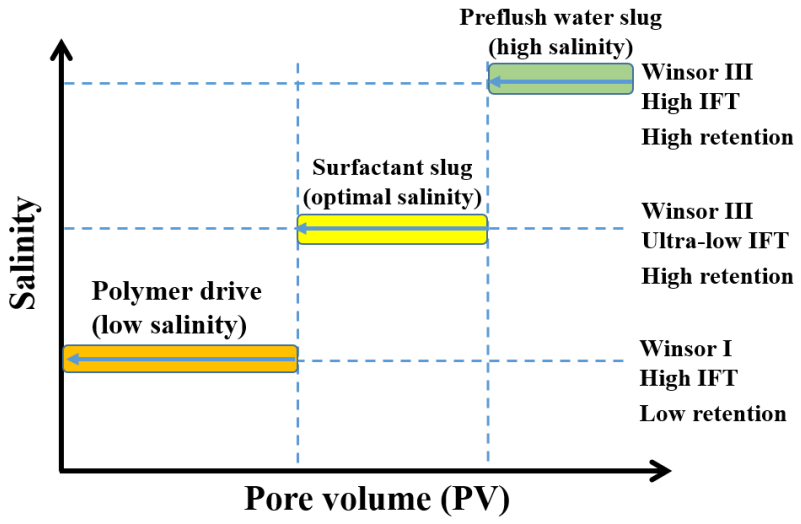

Figure 7. Schematic illustration of salinity gradient.

4.6 Low salinity water flooding

By lowering the total salinity and manipulating of ionic composition of the injected water, LS water flooding as a method for further EOR has been proven useful in both core plug and field scale tests.[42,208,300–304] The LS effect depends mainly on rock–fluid interactions and can be also explained by fluid–fluid interactions.[305,306] It should be noted that LS water flooding and smart water flooding are not distinguished here due to small difference in the controlled or specified ion composition. The combination of surfactant with LS water flooding has showed an improved oil recovery in comparison with only LS water flooding or only surfactant flooding.[200,201] A main advantage of the LS surfactant (LSS) flooding is the lower surfactant adsorption with ultralow IFT. Nourani et al. found that the flow of LSS solutions

on oil-coated aluminosilicate and silica surfaces decreased surfactant adsorption and increased oil desorption.[307] They also showed that an increase in surfactant concentration resulted in more wettability alteration of aluminosilicate surfaces toward water-wet, whereas silica surfaces kept relatively constant. Liu et al. applied QCM-D to investigate the salinity effect on surfactant adsorption, the lower adsorption of surfactants in LS than in high salinity solution stemmed from the less Ca^{2+} in LS.[53] Under LSS conditions, more QCM-D studies of the adsorption of desorption of crude oil or oil components (asphaltenes and resins) have been thoroughly investigated on solid surfaces, such as calcite, aluminosilicate, and silica surfaces.[75,201,308,309] With core flooding experiments, total surfactant content was analyzed by potentiometric titration and it was found that the average surfactant retention on Berea sandstone was 0.24 mg/g rock at a LS condition and 0.39 mg surfactant/g rock for the optimal salinity floods, both at 100% water saturation, and when oil was present.[200] With a decrease of Ca^{2+}/Na^{+} ratio, the alkylbenzene sulfonate adsorption decreased at 60 °C.[310] At lower Ca^{2+}/Na^{+} ratio, Khanamiri al et. also showed a reduction of surfactant adsorption, whereas CMC and IFT were higher.[311] Although the IFT was usually higher than the ultralow values, the LSS flooding resulted in additional oil recovery and very low surfactant retention.[312] Furthermore, the divalent cation to sulfate ion ratio (0-4.427) had a significant role in the adsorption of anionic surfactants and surfactant augmented NPs on clay containing rock surfaces, thus influencing the wettability of sandstone.[313]

5. Perspectives and challenges

Surfactant based EOR performs well at low salinity and low temperature conditions, and sandstone reservoirs. However, serious surfactant losses by adsorption rise in high salinity, high temperature, and carbonate reservoirs. Basically, these challenges need to be determined and solved before surfactant flooding is put into operation at harsh field conditions. Many

attempts have been made to mitigate surfactant adsorption and extend its applications which include:

(1) Alkalis: The major roles of alkalis in an ASP process are to minimize surfactant adsorption, sequester divalent ions, and also generate in situ soap. One of the principal problems in the alkali injection is the scale formation, especially in carbonate reservoirs with $CaSO_4$ and $CaSO_4 \cdot 2H_2O$. The alkali reacts with the rock and increases the concentration of scaling ions, such as Ca^{2+}, Mg^{2+}, Al^{3+}, Fe^{3+}, OH^-, CO_3^{2-}, SiO_3^{2-}, and SO_4^{2-}. These ions easily react to produce inorganic scales, thus reducing permeability, plugging production lines, and fouling equipment. Therefore, we need to answer two questions (i) how to reduce scaling formations? (ii) do advantages of alkalis addition outweigh disadvantages or whether alkalis have to be used? In the question (i), weaker alkalis like ammonia and $NaBO_2$, and organic alkalis are proposed to replace traditional NaOH and Na_2CO_3. Scale inhibitors are also used widely to tackle this problem.[80,167] Moreover, alkali-free SP flooding has been proposed.[235,314] Although the absence of alkalis might solve the scale formation, the surfactant adsorption issue exists and production costs probably increase. For the question (ii), it depends on the relative cost of alkalis to the benefits of the incremental oil recovery factors.

(2) Sacrificial agents: Addition of polyelectrolytes as the sacrificial agent to suppress the continuous adsorption of surfactants is mainly achieved by shielding adsorption sites of rocks and/or forming complexes with cations present in the hardness brine. This makes it possible to apply surfactants in higher salinities over 300,000 mg/l and higher temperature (100 ^oC) conditions, using polyelectrolytes such as PSS, PA, and EDTA.[79,250,252,262] However, the presence of $CaSO_4$ can reduce the effectiveness of PA as an sacrificial agent and this also holds true for EDTA with the sequestration of divalent cations.[179,250] The surfactant and polymer selections could be revisited to reduce the possible impact of $CaSO_4$. These sacrificial agents must also be cost effective.

(3) Nanofluids: A mixture of NPs and surfactants can help to reduce surfactant adsorption. However, NPs preferentially aggregate together and block pore throats because of their strong interactions, especially at high salinity and high temperature conditions.[315] Therefore, it is of great importance to create stable and homogeneous suspensions of NPs. Many researchers have been investigating the effect of different types of NPs (SiO_2, Al_2O_3, TiO_2, etc.), different coatings functionalized with polymers or surfactants, different solution compositions, and different NP compositions (nanocomposites). On the other hand, the novel concept of nanocarriers, nanocapsules, and nanodroplets are developing to make full use of surfactants and produce various types of nanofluids.

(4) High salinity: Strong surfactant adsorption is found at high salinity conditions irrespective of surfactant concentration. Pre-flushes with lower salinity brine or polymer slugs are widely applied to reduce surface loss and sequester divalent ions. More developments could focus on formulations of cheap (from waste and by-products) and efficient EOR surfactants, which show a greater tolerance to salinity. Moreover, the negative salinity gradient injection strategy can be chosen to mitigate surfactant adsorption and the salinity of injected surfactant solutions should be close to the optimum salinity. An EOR process combining LS and surfactant flooding has not only mitigated surfactant adsorption, but also shown a higher oil recovery compared to the methods on their own. However, it is not practicable to perform offshore LSS flooding where there is a lack of fresh water and only seawater (salinity 32,000-35,000 mg/L) or formation water is available.

(5) High temperature: Temperature is a crucial parameter to evaluate surfactant performance in a reservoir. Sheng summarized the reservoir temperature for surfactant flooding and found that most of researchers proposed 93.3 °C as a temperature limit, even though specific IOS surfactants were stable up to 150 °C.[21] Below 60 °C, sulfate surfactant generally considered stable and has a high salinity tolerance. Anionic carboxylate and sulfonate surfactants with

varying numbers of EO and PO groups, and hydrocarbon lengths have been proposed for high temperature (~100 °C), high salinity (~60,000 ppm) carbonate reservoirs.[179,229,316–318] Kamal et al. suggested amphoteric surfactants (hydroxyl betaine-based) were stable at 90 °C for 30 days and showed minimum adsorption (<1 mg/g rock) on carbonate reservoirs.[319] Biodegradable and renewable surfactants have also been developed, such as from non-edible Jatropha oil, agriculture material.[320–323] A good surfactant not only meets the requirements of high temperature stability, but also should satisfy other conditions to achieve a higher oil recovery in a cost-effective way, such as low surfactant adsorption and high solubilization ratios. When a single kind of surfactant does not successfully implement in high temperature reservoirs, a mixed surfactant system can be an appropriate alternative strategy.

6. Conclusions

Recent advances on surfactant adsorption on mineral surfaces in cEOR are reviewed. The adsorption behavior of surfactants is discussed with particular emphasis on adsorption mechanisms, isotherms, kinetics, thermodynamics, and adsorption structures. Surfactant adsorption mechanisms include electrostatic interactions (ion exchange/bridging), van der Waals interactions (London dispersion forces), acid-base interactions (hydrogen bonding, Lewis acid-base reactions), hydrophobic interactions, π electron polarizations, covalent bonding, and solvation of adsorbate species. Several of the above mentioned mechanisms contribute to the adsorption process, depending on the mineral and surfactant types, surfactant concentrations, ionic strengths, temperature, etc. To determine the amount of surfactant loss, four typical adsorption isotherms are mainly presented as well as other S-type, two/three-stage adsorption isotherms. The PFO, PSO, IPD, and Elovich kinetic models are frequently applied for surfactant adsorption. Taking considerations of the thermodynamic process are important to determine whether the adsorption process is spontaneous. The Van't Hoff equation should be used with care to derive thermodynamic parameters. The adsorbed

surfactant layers can be qualitatively and quantitatively analyzed by AFM, SE, QCM-D, SPR, as well as MD and DPD simulations.

Main factors influence surfactant adsorption, including (i) surfactant characteristics. Types of anionic, cationic, zwitterionic, and nonionic surfactants with different head groups, such as sulfonate and sulfate groups. Surfactant mixtures, surfactant structures with various functional groups (EO and PO), linear chain or branched chain, and surfactant concentrations; (ii) solution chemistry, *i.e.*, solution pH, ionic composition with monovalent and divalent cations, hardness and salinity; (iii) rock mineralogy referred to sandstones, carbonates, and unconventional shales; (iv) and reservoir temperature. In an effort to mitigate surfactant adsorption, various additives and chemical formulations have been proposed with the addition of alkalis (strong alkalis, weak alkalis, and organic alkalis), polymers (for example, PSS, PA, and EDTA), nanoparticles (SiO_2, Al_2O_3 and modified nanoparticles), co-solvents, ionic liquids as well as implementing with salinity gradient and low salinity water flooding strategies. Finally, current trends and future challenges in alkalis, sacrificial agents, nanofluids injections, at high salinity and high temperature conditions for surfactant based EOR are outlined, which significantly improve our knowledge in designing and optimizing cEOR with reduced surfactant loss.

Conflict of interests

The authors declare no competing financial interest.

Acknowledgments

The authors thank Dr. John van Wunnik, and Dr. Dirk Groenendijk (Shell Global Solutions) for their active discussions and careful corrections. This work was supported by the Shell Global Solutions, Science Foundation of China University of Petroleum, Beijing (no.

2462020BJRC007, 2462020YXZZ003), and Major Science and Technology Project of Shanxi Province (no. 20181101013, 20201102002).

Nomenclature

Abbreviations

AAS	alcohol alkoxy sulfate
AEC	alkyl ether carboxylate
AFM	atomic force microscope
AOS	alpha olefin sulfonates
APCA	aminopolycarboxylic acid
ASP	alkaline-surfactant-polymer
BTAC	behenyl trimethyl ammonium chloride
$CaCO_3$	calcite or aragonite (less stable crystal form of $CaCO_3$)
$CaMg(CO_3)_2$	dolomite
$CaSO_4$	anhydrite
$CaSO_4 \cdot 2H_2O$	gypsum
$C_{12}E_6$	hexaethylene glycol monododecyl ether
cEOR	chemical EOR
CMC	critical micelle concentration
$-COO^-$	carboxylate
CTAB	cetyltrimethyl ammonium bromide
CTAC	hexadecyltrimethyl ammonium chloride
CTVB	alkyl trimethylammonium vinylbenzoate
DES	deep eutectic solvent
DICL	dodecylamine hydrochloride
DPD	dissipative particle dynamics
DTAB	dodecyltrimethylammonium bromide
DTPA	diethylenetriaminepentaacetic acid
EA	ethanolamine
EDTA	ethylenediaminetetraacetic acid
EO	ethylene oxide
EOR	enhanced oil recovery
^{1}H-NMR	proton nuclear magnetic resonance spectroscopy
HS-AFM	high-speed AFM
IBA	iso-butanol
IEP	isoelectric point
IFT	interfacial tension
ILs	ionic liquids
IPD	intra particle diffusion
IOS	internal olefin sulfonate
LS	low salinity
LSS	LS surfactant
$MgCO_3$	magnesite
MD	molecular dynamics
MW	molecular weight
Na_2CO_3	sodium carbonate (soda ash)
$NaHCO_3$	sodium bicarbonate
$NaBO_2$	sodium metaborate
$Na_2B_4O_7$	sodium tetraborate
NaOH	sodium hydroxide (caustic soda)
Na_3PO_4	sodium phosphate
Na_4SiO_4	sodium orthosilicate

NH_4OH	ammonium hydroxide
NP	nanoparticle
NPE10	nonylphenol ethoxylate
OOIP	original oil in place
PA	polyacrylate
PASC1	acryloyloxyethyl-N, Ndimethyl-N-octylammonium bromide
PFO	pseudo-first-order
PO	propoxy (C_3H_6O)
PSO	pseudo-second-order
PSS	polystyrene sulfonate
PVP	poly(vinylpyrrolidone)
QAC	quaternary ammonium compounds
QCM-D	quartz crystal microbalance with dissipation monitoring
$-SO_4^{2-}$	sulfate
$-SO_3^-$	sulfonate
SiO_2	silica
SD	standard deviation
SDS	sodium dodecyl sulfate
SDBS	sodium dodecylbenzene sulfonate
SE	spectroscopic ellipsometry
SFS	sum-frequency spectroscopy
SNP	silica NP
SPAM	sulfonated polyacrylamide
SPR	surface plasmon resonance
TDS	totally dissolved solids
TX-100	4-octylphenol polyethoxylated
Tween 20	polyoxyethylenesorbitan monolaurate
TIR	Raman total internal reflection Raman scattering
β-CD	beta-cyclodextrin

Variables

B	a constant related to the heat of adsorption
C	equilibrium surfactant concentration
T	absolute temperature in Kelvin (K)
R	the universal gas constant (8.314 $J/mol\ K$)
N_c	capillary number
K_L	the Langmuir equilibrium constant
K_F	the Freundlich constant
K_T	the Temkin constant
K_R	the Redlich-Peterson constant
K_1	the equilibrium rate constant of the PFO model
K_2	the equilibrium rate constant of PSO model
K_i	equilibrium rate constant of IPD model
K°	the equilibrium constant
ΔG°	Gibbs free energy change
ΔS°	entropy
ΔH°	enthalpy
c	a constant related to the adsorption step
α	the initial adsorption rate
h	initial adsorption rate

1	n	the heterogeneity factor
2	τ	the activity coefficient
3	θ	the contact angle
4	μ	viscosity of the displacing liquid
5	v	velocity of the displacing liquid
6	γ	the IFT between oil and water
7	γ_1	the desorption constant
8	q_e	the equilibrium adsorption
9	q_m	the maximum amount of surfactant adsorption
10	q_t	the amount of surfactant adsorbed at time t
11	$t_{1/2}$	half-adsorption time

References

(1) Council, W. E. World Energy Scenarios 2019. *Word Energy Counc. Lond. UK* **2019**, *1*.

(2) Sheng, J. J. *Modern Chemical Enhanced Oil Recovery: Theory and Practice*; Gulf Professional Publishing, 2010.

(3) Howe, A. M.; Clarke, A.; Mitchell, J.; Staniland, J.; Hawkes, L.; Whalan, C. Visualising Surfactant Enhanced Oil Recovery. *Colloids Surf. Physicochem. Eng. Asp.* **2015**, *480*, 449–461.

(4) Mandal, A. Chemical Flood Enhanced Oil Recovery: A Review. *Int. J. Oil Gas Coal Technol.* **2015**, *9* (3), 241–264.

(5) Gbadamosi, A. O.; Junin, R.; Manan, M. A.; Agi, A.; Yusuff, A. S. An Overview of Chemical Enhanced Oil Recovery: Recent Advances and Prospects. *Int. Nano Lett.* **2019**, 1–32.

(6) Demirbas, A.; Alsulami, H. E.; Hassanein, W. S. Utilization of Surfactant Flooding Processes for Enhanced Oil Recovery (EOR). *Pet. Sci. Technol.* **2015**, *33* (12), 1331–1339.

(7) Al Adasani, A.; Bai, B. Analysis of EOR Projects and Updated Screening Criteria. *J. Pet. Sci. Eng.* **2011**, *79* (1–2), 10–24.

(8) Wever, D. A. Z.; Picchioni, F.; Broekhuis, A. A. Polymers for Enhanced Oil Recovery: A Paradigm for Structure–Property Relationship in Aqueous Solution. *Prog. Polym. Sci.* **2011**, *36* (11), 1558–1628.

(9) Kamal, M. S.; Sultan, A. S.; Hussein, I. A. Screening of Amphoteric and Anionic Surfactants for CEOR Applications Using a Novel Approach. *Colloids Surf. Physicochem. Eng. Asp.* **2015**, *476*, 17–23.

(10) Bera, A.; Kumar, T.; Ojha, K.; Mandal, A. Screening of Microemulsion Properties for Application in Enhanced Oil Recovery. *Fuel* **2014**, *121*, 198–207.

(11) Kamal, M. S.; Hussein, I. A.; Sultan, A. S. Review on Surfactant Flooding: Phase Behavior, Retention, IFT, and Field Applications. *Energy Fuels* **2017**, *31* (8), 7701–7720.

(12) Bera, A.; Kumar, T.; Ojha, K.; Mandal, A. Adsorption of Surfactants on Sand Surface in Enhanced Oil Recovery: Isotherms, Kinetics and Thermodynamic Studies. *Appl. Surf. Sci.* **2013**, *284*, 87–99.

(13) Wesson, L. L.; Harwell, J. H. Surfactant Adsorption in Porous Media. *Surfactants Fundam. Appl. Pet. Ind.* **2000**, 121–158.

(14) Kamal, M. S.; Sultan, A. S.; Al-Mubaiyedh, U. A.; Hussein, I. A. Review on Polymer Flooding: Rheology, Adsorption, Stability, and Field Applications of Various Polymer Systems. *Polym. Rev.* **2015**, *55* (3), 491–530.

(15) Hirasaki, G.; Zhang, D. L. Surface Chemistry of Oil Recovery from Fractured, Oil-Wet, Carbonate Formations. *Spe J.* **2004**, *9* (02), 151–162.

(16) Tackie-Otoo, B. N.; Mohammed, M. A. A.; Yekeen, N.; Negash, B. M. Alternative Chemical Agents for Alkalis, Surfactants and Polymers for Enhanced Oil Recovery: Research Trend and Prospects. *J. Pet. Sci. Eng.* **2020**, *187*, 106828.

(17) Ayirala, S. C.; Rao, D. N. Multiphase Flow and Wettability Effects of Surfactants in Porous Media. *Colloids Surf. Physicochem. Eng. Asp.* **2004**, *241* (1–3), 313–322.

(18) Nwidee, L. N.; Theophilus, S.; Barifcani, A.; Sarmadivaleh, M.; Iglauer, S. EOR Processes, Opportunities and Technological Advancements. *Chem. Enhanc. Oil Recovery CEOR- Pract. Overv.* **2016**, 2–52.

(19) Hou, J.; Liu, Z.; Zhang, S.; Yang, J. The Role of Viscoelasticity of Alkali/Surfactant/Polymer Solutions in Enhanced Oil Recovery. *J. Pet. Sci. Eng.* **2005**, *47* (3–4), 219–235.

(20) Spildo, K.; Johannessen, A. M.; Skauge, A. Low Salinity Waterflood at Reduced Capillarity. In *SPE Improved Oil Recovery Symposium*; Society of Petroleum Engineers, 2012.

(21) Sheng, J. J. Status of Surfactant EOR Technology. *Petroleum* **2015**, *1* (2), 97–105.

(22) Ahmadi, M. A.; Shadizadeh, S. R. Implementation of a High-Performance Surfactant for Enhanced Oil Recovery from Carbonate Reservoirs. *J. Pet. Sci. Eng.* **2013**, *110*, 66–73.

(23) Iglauer, S.; Rahman, T.; Sarmadivaleh, M.; Al-Hinai, A.; Fernø, M. A.; Lebedev, M. Influence of Wettability on Residual Gas Trapping and Enhanced Oil Recovery in Three-Phase Flow: A Pore-Scale Analysis by Use of Microcomputed Tomography. *SPE J.* **2016**, *21* (06), 1,916-1,929.

(24) Mohammed, M.; Babadagli, T. Wettability Alteration: A Comprehensive Review of Materials/Methods and Testing the Selected Ones on Heavy-Oil Containing Oil-Wet Systems. *Adv. Colloid Interface Sci.* **2015**, *220*, 54–77.
(25) Fu, L.; Zhang, G.; Ge, J.; Liao, K.; Pei, H.; Jiang, P.; Li, X. Study on Organic Alkali-Surfactant-Polymer Flooding for Enhanced Ordinary Heavy Oil Recovery. *Colloids Surf. Physicochem. Eng. Asp.* **2016**, *508*, 230–239.
(26) Ahmadi, M. A.; Galedarzadeh, M.; Shadizadeh, S. R. Wettability Alteration in Carbonate Rocks by Implementing New Derived Natural Surfactant: Enhanced Oil Recovery Applications. *Transp. Porous Media* **2015**, *106* (3), 645–667.
(27) Murillo-Hernández, J. A.; García-Cruz, I.; Lopez-Ramirez, S.; Duran-Valencia, C.; Domínguez, J. M.; Aburto, J. Aggregation Behavior of Heavy Crude Oil− Ionic Liquids Solutions by Fluorescence Spectroscopy. *Energy Fuels* **2009**, *23* (9), 4584–4592.
(28) Vallejo-Cardona, A. A.; Cerón-Camacho, R.; Karamath, J. R.; Martínez-Palou, R.; Aburto, J. A Study of the Effect of Surfactants on the Aggregation Behavior of Crude Oil Aqueous Dispersions through Steady-State Fluorescence Spectrometry. *Appl. Spectrosc.* **2017**, *71* (7), 1519–1529.
(29) Gong, L.; Liao, G.; Luan, H.; Chen, Q.; Nie, X.; Liu, D.; Feng, Y. Oil Solubilization in Sodium Dodecylbenzenesulfonate Micelles: New Insights into Surfactant Enhanced Oil Recovery. *J. Colloid Interface Sci.* **2020**, *569*, 219–228.
(30) Bhui, U. K.; Sanyal, S.; Saha, R.; Rakshit, S.; Pal, S. K. Steady-State and Time-Resolved Fluorescence Spectroscopic Study of Petroleum Crudes in Aqueous-Surfactant Solutions: Its Implications for Enhanced Oil Recovery (EOR) during Surfactant Flooding. *Fuel* **2018**, *234*, 1081–1088.
(31) Anto, A.; Sanyal, S.; Bhattacharjee, S.; Bhui, U. K. Optical Characteristics of Petroleum Crudes–Surfactant–Brine Solutions: Understanding Molecular Level Interaction for Designing Injection Fluids for Enhanced Oil Recovery. *Macromol. Charact. Hydrocarb. Sustain. Future Appl. Hydrocarb. Value Chain* **2020**, 59.
(32) Kumar, A.; Mandal, A. Characterization of Rock-Fluid and Fluid-Fluid Interactions in Presence of a Family of Synthesized Zwitterionic Surfactants for Application in Enhanced Oil Recovery. *Colloids Surf. Physicochem. Eng. Asp.* **2018**, *549*, 1–12.
(33) Valluri, M. K.; Alvarez, J. O.; Schechter, D. S. Study of the Rock/Fluid Interactions of Sodium and Calcium Brines with Ultra-Tight Rock Surfaces and Their Impact on Improving Oil Recovery by Spontaneous Imbibition. In *SPE Low Perm Symposium*; Society of Petroleum Engineers, 2016.
(34) Goudarzi, A.; Delshad, M.; Mohanty, K. K.; Sepehrnoori, K. Surfactant Oil Recovery in Fractured Carbonates: Experiments and Modeling of Different Matrix Dimensions. *J. Pet. Sci. Eng.* **2015**, *125*, 136–145.
(35) Karambeigi, M. S.; Abbassi, R.; Roayaei, E.; Emadi, M. A. Emulsion Flooding for Enhanced Oil Recovery: Interactive Optimization of Phase Behavior, Microvisual and Core-Flood Experiments. *J. Ind. Eng. Chem.* **2015**, *29*, 382–391.
(36) Belhaj, A. F.; Elraies, K. A.; Mahmood, S. M.; Zulkifli, N. N.; Akbari, S.; Hussien, O. S. The Effect of Surfactant Concentration, Salinity, Temperature, and PH on Surfactant Adsorption for Chemical Enhanced Oil Recovery: A Review. *J. Pet. Explor. Prod. Technol.* **2019**, 1–13.
(37) Zhang, R.; Somasundaran, P. Advances in Adsorption of Surfactants and Their Mixtures at Solid/Solution Interfaces. *Adv. Colloid Interface Sci.* **2006**, *123*, 213–229.
(38) Olajire, A. A. Review of ASP EOR (Alkaline Surfactant Polymer Enhanced Oil Recovery) Technology in the Petroleum Industry: Prospects and Challenges. *Energy* **2014**, *77*, 963–982.
(39) Almahfood, M.; Bai, B. The Synergistic Effects of Nanoparticle-Surfactant Nanofluids in EOR Applications. *J. Pet. Sci. Eng.* **2018**, *171*, 196–210.
(40) Ahmadi, M.; Chen, Z. Challenges and Future of Chemical Assisted Heavy Oil Recovery Processes. *Adv. Colloid Interface Sci.* **2019**, 102081.
(41) Hirasaki, G.; Miller, C. A.; Puerto, M. Recent Advances in Surfactant EOR. *SPE J.* **2011**, *16* (04), 889–907.
(42) Lager, A.; Webb, K. J.; Black, C. J. J. Impact of Brine Chemistry on Oil Recovery. In *IOR 2007-14th European Symposium on Improved Oil Recovery*; 2007.

(43) Elias, S. D.; Rabiu, A. M.; Oluwaseun, O.; Seima, B. Adsorption Characteristics of Surfactants on Different Petroleum Reservoir Materials. **2016**.
(44) Park, S.; Lee, E. S.; Sulaiman, W. R. W. Adsorption Behaviors of Surfactants for Chemical Flooding in Enhanced Oil Recovery. *J. Ind. Eng. Chem.* **2015**, *21*, 1239–1245.
(45) Barati, A.; Najafi, A.; Daryasafar, A.; Nadali, P.; Moslehi, H. Adsorption of a New Nonionic Surfactant on Carbonate Minerals in Enhanced Oil Recovery: Experimental and Modeling Study. *Chem. Eng. Res. Des.* **2016**, *105*, 55–63.
(46) Tiberg, F.; Brinck, J.; Grant, L. Adsorption and Surface-Induced Self-Assembly of Surfactants at the Solid–Aqueous Interface. *Curr. Opin. Colloid Interface Sci.* **1999**, *4* (6), 411–419.
(47) Striolo, A. Studying Surfactants Adsorption on Heterogeneous Substrates. *Curr. Opin. Chem. Eng.* **2019**, *23*, 115–122.
(48) Hamon, J. J.; Tabor, R. F.; Striolo, A.; Grady, B. P. Atomic Force Microscopy Force Mapping Analysis of an Adsorbed Surfactant above and below the Critical Micelle Concentration. *Langmuir* **2018**, *34* (25), 7223–7239.
(49) Kou, J.; Xu, S.; Sun, T.; Sun, C.; Guo, Y.; Wang, C. A Study of Sodium Oleate Adsorption on Ca2+ Activated Quartz Surface Using Quartz Crystal Microbalance with Dissipation. *Int. J. Miner. Process.* **2016**, *154*, 24–34.
(50) Sakai, K.; Matsuhashi, K.; Honya, A.; Oguchi, T.; Sakai, H.; Abe, M. Adsorption Characteristics of Monomeric/Gemini Surfactant Mixtures at the Silica/Aqueous Solution Interface. *Langmuir* **2010**, *26* (22), 17119–17125.
(51) Liu, J.-F.; Min, G.; Ducker, W. A. AFM Study of Adsorption of Cationic Surfactants and Cationic Polyelectrolytes at the Silica− Water Interface. *Langmuir* **2001**, *17* (16), 4895–4903.
(52) Koizumi, K.; Akamatsu, M.; Sakai, K.; Sasaki, S.; Sakai, H. Real-Time Observation of Solubilization-Induced Morphological Change in Surfactant Aggregates Adsorbed on a Solid Surface. *Chem. Commun.* **2017**, *53* (98), 13172–13175.
(53) Liu, Z.; Ghatkesar, M. K.; Sudholter, E. J.; Singh, B.; Kumar, N. Understanding the Cation Dependent Surfactant Adsorption on Clay Minerals in Oil Recovery. *Energy Fuels* **2019**, *33* (12), 12319–12329.
(54) Haaring, R. M.; Kumar, N.; Bosma, D.; Poltorak, L.; Sudholter, E. J. Electrochemically-Assisted Deposition of Calcite for Application in Surfactant Adsorption Studies. *Energy Fuels* **2019**.
(55) Kou, J.; Tao, D.; Xu, G. A Study of Adsorption of Dodecylamine on Quartz Surface Using Quartz Crystal Microbalance with Dissipation. *Colloids Surf. Physicochem. Eng. Asp.* **2010**, *368* (1–3), 75–83.
(56) Zhou, X.; Liang, J.-T.; Andersen, C. D.; Cai, J.; Lin, Y.-Y. Enhanced Adsorption of Anionic Surfactants on Negatively Charged Quartz Sand Grains Treated with Cationic Polyelectrolyte Complex Nanoparticles. *Colloids Surf. Physicochem. Eng. Asp.* **2018**, *553*, 397–405.
(57) Kou, J.; Xu, S. In Situ Kinetics and Conformation Studies of Dodecylamine Adsorption onto Zinc Sulfide Using a Quartz Crystal Microbalance with Dissipation (QCM-D). *Colloids Surf. Physicochem. Eng. Asp.* **2016**, *490*, 110–120.
(58) Medina, S. C.; Farinha, A. S.; Emwas, A.-H.; Tabatabai, A.; Leiknes, T. A Fundamental Study of Adsorption Kinetics of Surfactants onto Metal Oxides Using Quartz Crystal Microbalance with Dissipation (QCM-D). *Colloids Surf. Physicochem. Eng. Asp.* **2020**, *586*, 124237.
(59) Thavorn, J.; Hamon, J. J.; Kitiyanan, B.; Striolo, A.; Grady, B. P. Competitive Surfactant Adsorption of AOT and Tween 20 on Gold Measured Using a Quartz Crystal Microbalance with Dissipation. *Langmuir* **2014**, *30* (37), 11031–11039.
(60) Chen, Y.-L.; Zhang, L.; Song, J.; Jian, G.; Hirasaki, G.; Johnston, K.; Biswal, S. L. Two-Step Adsorption of a Switchable Tertiary Amine Surfactant Measured Using a Quartz Crystal Microbalance with Dissipation. *Langmuir* **2019**, *35* (3), 695–701.
(61) Benoit, D.; Saputra, I.; Recio III, A.; Henkel-Holan, K. Investigating the Role of Surfactant in Oil/Water/Rock Systems Using QCM-D. In *SPE International Conference and Exhibition on Formation Damage Control*; Society of Petroleum Engineers, 2020.
(62) Liu, Z.; Onay, H.; Guo, F.; Chen, J.; Poltorak, L.; Hedayati, P.; Sudhölter, E. J. Calcium Carbonate-Modified Surfaces by Electrocrystallization To Study Anionic Surfactant Adsorption. *Energy Fuels* **2021**, *35* (2), 1358–1370.

(63) Richter, R. P.; Rodenhausen, K. B.; Eisele, N. B.; Schubert, M. Coupling Spectroscopic Ellipsometry and Quartz Crystal Microbalance to Study Organic Films at the Solid-Liquid Interface. In *Ellipsometry of functional organic surfaces and films*; Springer, 2014; pp 223–248.
(64) Fang, J.; Ren, C.; Zhu, T.; Wang, K.; Jiang, Z.; Ma, Y. Comparison of the Different Responses of Surface Plasmon Resonance and Quartz Crystal Microbalance Techniques at Solid–Liquid Interfaces under Various Experimental Conditions. *Analyst* **2015**, *140* (4), 1323–1336.
(65) Mivehi, L.; Bordes, R.; Holmberg, K. Adsorption of Cationic Gemini Surfactants at Solid Surfaces Studied by QCM-D and SPR: Effect of the Rigidity of the Spacer. *Langmuir* **2011**, *27* (12), 7549–7557.
(66) Höök, F.; Kasemo, B.; Nylander, T.; Fant, C.; Sott, K.; Elwing, H. Variations in Coupled Water, Viscoelastic Properties, and Film Thickness of a Mefp-1 Protein Film during Adsorption and Cross-Linking: A Quartz Crystal Microbalance with Dissipation Monitoring, Ellipsometry, and Surface Plasmon Resonance Study. *Anal. Chem.* **2001**, *73* (24), 5796–5804.
(67) Liu, Q.; Dong, M.; Zhou, W.; Ayub, M.; Zhang, Y. P.; Huang, S. Improved Oil Recovery by Adsorption–Desorption in Chemical Flooding. *J. Pet. Sci. Eng.* **2004**, *43* (1–2), 75–86.
(68) Amirianshoja, T.; Junin, R.; Idris, A. K.; Rahmani, O. A Comparative Study of Surfactant Adsorption by Clay Minerals. *J. Pet. Sci. Eng.* **2013**, *101*, 21–27.
(69) Dang, C. T. Q.; Chen, Z. J.; Nguyen, N. T. B.; Bae, W.; Phung, T. H. Development of Isotherm Polymer/Surfactant Adsorption Models in Chemical Flooding. In *SPE Asia Pacific oil and gas conference and exhibition*; Society of Petroleum Engineers, 2011.
(70) Han, M.; AlSofi, A.; Fuseni, A.; Zhou, X.; Hassan, S. Development of Chemical EOR Formulations for a High Temperature and High Salinity Carbonate Reservoir. In *IPTC 2013: International Petroleum Technology Conference*; European Association of Geoscientists & Engineers, 2013; p cp-350-00486.
(71) Somasundaran, P.; Huang, L. Adsorption/Aggregation of Surfactants and Their Mixtures at Solid–Liquid Interfaces. *Adv. Colloid Interface Sci.* **2000**, *88* (1–2), 179–208.
(72) Paria, S.; Khilar, K. C. A Review on Experimental Studies of Surfactant Adsorption at the Hydrophilic Solid–Water Interface. *Adv. Colloid Interface Sci.* **2004**, *110* (3), 75–95.
(73) Rosen, M. J.; Kunjappu, J. T. Adsorption of Surface-Active Agents at Interfaces: The Electrical Double Layer. *Surfactants Interfacial Phenom.* **2004**, *4*, 98.
(74) Farooq, U.; Tweheyo, M. T.; Sjöblom, J.; Øye, G. Surface Characterization of Model, Outcrop, and Reservoir Samples in Low Salinity Aqueous Solutions. *J. Dispers. Sci. Technol.* **2011**, *32* (4), 519–531.
(75) Al-Khafaji, A.; Neville, A.; Wilson, M.; Wen, D. Effect of Low Salinity on the Oil Desorption Efficiency from Calcite and Silica Surfaces. *Energy Fuels* **2017**, *31* (11), 11892–11901.
(76) Kosmulski, M. Positive Electrokinetic Charge of Silica in the Presence of Chlorides. *J. Colloid Interface Sci.* **1998**, *208* (2), 543–545.
(77) Labidi, N. S. Studies of the Mechanism of Polyvinyl Alcohol Adsorption on the Calcite/Water Interface in the Presence of Sodium Oleate. *J. Miner. Mater. Charact. Eng.* **2008**, *7* (02), 147.
(78) Al Mahrouqi, D.; Vinogradov, J.; Jackson, M. D. Zeta Potential of Artificial and Natural Calcite in Aqueous Solution. *Adv. Colloid Interface Sci.* **2017**, *240*, 60–76.
(79) ShamsiJazeyi, H.; Verduzco, R.; Hirasaki, G. J. Reducing Adsorption of Anionic Surfactant for Enhanced Oil Recovery: Part II. Applied Aspects. *Colloids Surf. Physicochem. Eng. Asp.* **2014**, *453*, 168–175.
(80) Pal, S.; Mushtaq, M.; Banat, F.; Al Sumaiti, A. M. Review of Surfactant-Assisted Chemical Enhanced Oil Recovery for Carbonate Reservoirs: Challenges and Future Perspectives. *Pet. Sci.* **2018**, *15* (1), 77–102.
(81) Solairaj, S.; Britton, C.; Kim, D. H.; Weerasooriya, U.; Pope, G. A. Measurement and Analysis of Surfactant Retention. In *SPE Improved Oil Recovery Symposium*; Society of Petroleum Engineers, 2012.
(82) Barati-Harooni, A.; Najafi-Marghmaleki, A.; Tatar, A.; Mohammadi, A. H. Experimental and Modeling Studies on Adsorption of a Nonionic Surfactant on Sandstone Minerals in Enhanced Oil Recovery Process with Surfactant Flooding. *J. Mol. Liq.* **2016**, *220*, 1022–1032.

(83) Jong, K.; Han, Y.; Ryom, S. Flotation Mechanism of Oleic Acid Amide on Apatite. *Colloids Surf. Physicochem. Eng. Asp.* **2017**, *523*, 127–131.
(84) Lima, É. C.; Adebayo, M. A.; Machado, F. M. Kinetic and Equilibrium Models of Adsorption. In *Carbon nanomaterials as adsorbents for environmental and biological applications*; Springer, 2015; pp 33–69.
(85) Lebouachera, S. E. I.; Chemini, R.; Khodja, M.; Grassl, B.; Tassalit, D.; Drouiche, N. Experimental Investigations of SDS Adsorption on the Algerian Rock Reservoir: Chemical Enhanced Oil Recovery Case. *Res. Chem. Intermed.* **2018**, *44* (12), 7665–7690.
(86) Ahmadi, M. A.; Shadizadeh, S. R. Experimental Investigation of a Natural Surfactant Adsorption on Shale-Sandstone Reservoir Rocks: Static and Dynamic Conditions. *Fuel* **2015**, *159*, 15–26.
(87) Ayad, M. M.; El-Nasr, A. A. Adsorption of Cationic Dye (Methylene Blue) from Water Using Polyaniline Nanotubes Base. *J. Phys. Chem. C* **2010**, *114* (34), 14377–14383.
(88) Weber, T. W.; Chakravorti, R. K. Pore and Solid Diffusion Models for Fixed-bed Adsorbers. *AIChE J.* **1974**, *20* (2), 228–238.
(89) Tehrani-Bagha, A. R.; Holmberg, K. Cationic Ester-Containing Gemini Surfactants: Adsorption at Tailor-Made Surfaces Monitored by SPR and QCM. *Langmuir* **2008**, *24* (12), 6140–6145.
(90) Ebaga-Ololo, J.; Chon, B. Static Adsorption of Dodecyl Alkyl Sulfate onto Kaolinite: An Experimental Investigation for Enhanced Oil Recovery Purposes. *Int. J. Appl. Eng. Res.* **2018**, *13* (19), 14438–14446.
(91) Liu, Z.; Hedayati, P.; Sudhölter, E. J.; Haaring, R.; Shaik, A. R.; Kumar, N. Adsorption Behavior of Anionic Surfactants to Silica Surfaces in the Presence of Calcium Ion and Polystyrene Sulfonate. *Colloids Surf. Physicochem. Eng. Asp.* **2020**, 125074.
(92) Rosen, M. J.; Kunjappu, J. T. *Surfactants and Interfacial Phenomena*; John Wiley & Sons, 2012.
(93) Moslemizadeh, A.; Dehkordi, A. F.; Barnaji, M. J.; Naseri, M.; Ravi, S. G.; Jahromi, E. K. Novel Bio-Based Surfactant for Chemical Enhanced Oil Recovery in Montmorillonite Rich Reservoirs: Adsorption Behavior, Interaction Impact, and Oil Recovery Studies. *Chem. Eng. Res. Des.* **2016**, *109*, 18–31.
(94) Samiey, B.; Dargahi, M. Kinetics and Thermodynamics of Adsorption of Congo Red on Cellulose. *Open Chem.* **2010**, *8* (4), 906–912.
(95) Temkin, M. J.; Pyzhev, V. Recent Modifications to Langmuir Isotherms. **1940**.
(96) Wu, F.-C.; Liu, B.-L.; Wu, K.-T.; Tseng, R.-L. A New Linear Form Analysis of Redlich–Peterson Isotherm Equation for the Adsorptions of Dyes. *Chem. Eng. J.* **2010**, *162* (1), 21–27.
(97) Curbelo, F. D.; Santanna, V. C.; Neto, E. L. B.; Dutra Jr, T. V.; Dantas, T. N. C.; Neto, A. A. D.; Garnica, A. I. Adsorption of Nonionic Surfactants in Sandstones. *Colloids Surf. Physicochem. Eng. Asp.* **2007**, *293* (1–3), 1–4.
(98) Saxena, N.; Kumar, A.; Mandal, A. Adsorption Analysis of Natural Anionic Surfactant for Enhanced Oil Recovery: The Role of Mineralogy, Salinity, Alkalinity and Nanoparticles. *J. Pet. Sci. Eng.* **2019**, *173*, 1264–1283.
(99) Foo, K. Y.; Hameed, B. H. Insights into the Modeling of Adsorption Isotherm Systems. *Chem. Eng. J.* **2010**, *156* (1), 2–10.
(100) Ayawei, N.; Ebelegi, A. N.; Wankasi, D. Modelling and Interpretation of Adsorption Isotherms. *J. Chem.* **2017**, *2017*.
(101) Somasundaran, P.; Zhang, L. Adsorption of Surfactants on Minerals for Wettability Control in Improved Oil Recovery Processes. *J. Pet. Sci. Eng.* **2006**, *52* (1–4), 198–212.
(102) Chang, Z.; Chen, X.; Peng, Y. The Adsorption Behavior of Surfactants on Mineral Surfaces in the Presence of Electrolytes–A Critical Review. *Miner. Eng.* **2018**, *121*, 66–76.
(103) Chandar, P.; Somasundaran, P.; Turro, N. J. Fluorescence Probe Studies on the Structure of the Adsorbed Layer of Dodecyl Sulfate at the Alumina—Water Interface. *J. Colloid Interface Sci.* **1987**, *117* (1), 31–46.
(104) Fan, A.; Somasundaran, P.; Turro, N. J. Adsorption of Alkyltrimethylammonium Bromides on Negatively Charged Alumina. *Langmuir* **1997**, *13* (3), 506–510.

(105) Hodges, C.; Biggs, S.; Walker, L. Adsorption Studies of a Polymerizable Surfactant by Optical Reflectivity and Quartz Crystal Microbalance. *Langmuir* **2009**, *25* (19), 11503–11508.
(106) Atkin, R.; Craig, V. S.; Wanless, E. J.; Biggs, S. Mechanism of Cationic Surfactant Adsorption at the Solid–Aqueous Interface. *Adv. Colloid Interface Sci.* **2003**, *103* (3), 219–304.
(107) Gao, Y.; Du, J.; Gu, T. Hemimicelle Formation of Cationic Surfactants at the Silica Gel–Water Interface. *J. Chem. Soc. Faraday Trans. 1 Phys. Chem. Condens. Phases* **1987**, *83* (8), 2671–2679.
(108) Lagergren, S.; Lagergren, S.; Lagergren, S. Y.; Sven, K. Zurtheorie Der Sogenannten Adsorption Gelösterstoffe. **1898**.
(109) Simonin, J.-P. On the Comparison of Pseudo-First Order and Pseudo-Second Order Rate Laws in the Modeling of Adsorption Kinetics. *Chem. Eng. J.* **2016**, *300*, 254–263.
(110) Ho, Y.-S.; McKay, G. Pseudo-Second Order Model for Sorption Processes. *Process Biochem.* **1999**, *34* (5), 451–465.
(111) Ungarish, M.; Aharoni, C. Kinetics of Chemisorption. Deducing Kinetic Laws from Experimental Data. *J. Chem. Soc. Faraday Trans. 1 Phys. Chem. Condens. Phases* **1981**, *77* (5), 975–985.
(112) Febrianto, J.; Kosasih, A. N.; Sunarso, J.; Ju, Y.-H.; Indraswati, N.; Ismadji, S. Equilibrium and Kinetic Studies in Adsorption of Heavy Metals Using Biosorbent: A Summary of Recent Studies. *J. Hazard. Mater.* **2009**, *162* (2–3), 616–645.
(113) McKay, G.; Ho, Y. S.; Ng, J. C. Y. Biosorption of Copper from Waste Waters: A Review. *Sep. Purif. Methods* **1999**, *28* (1), 87–125.
(114) Ho, Y.-S. Review of Second-Order Models for Adsorption Systems. *J. Hazard. Mater.* **2006**, *136* (3), 681–689.
(115) Azizian, S. Kinetic Models of Sorption: A Theoretical Analysis. *J. Colloid Interface Sci.* **2004**, *276* (1), 47–52.
(116) Allen, S. J.; Gan, Q.; Matthews, R.; Johnson, P. A. Kinetic Modeling of the Adsorption of Basic Dyes by Kudzu. *J. Colloid Interface Sci.* **2005**, *286* (1), 101–109.
(117) Weber, W. J.; Morris, J. C. Kinetics of Adsorption on Carbon from Solution. *J. Sanit. Eng. Div.* **1963**, *89* (2), 31–60.
(118) Nazari, G.; Abolghasemi, H.; Esmaieli, M. Batch Adsorption of Cephalexin Antibiotic from Aqueous Solution by Walnut Shell-Based Activated Carbon. *J. Taiwan Inst. Chem. Eng.* **2016**, *58*, 357–365.
(119) Kajjumba, G. W.; Emik, S.; Öngen, A.; Özcan, H. K.; Aydın, S. Modelling of Adsorption Kinetic Processes—Errors, Theory and Application. In *Advanced sorption process applications*; IntechOpen, 2018.
(120) Tang, B.; Lin, Y.; Yu, P.; Luo, Y. Study of Aniline/ε-Caprolactam Mixture Adsorption from Aqueous Solution onto Granular Activated Carbon: Kinetics and Equilibrium. *Chem. Eng. J.* **2012**, *187*, 69–78.
(121) Malash, G. F.; El-Khaiary, M. I. Piecewise Linear Regression: A Statistical Method for the Analysis of Experimental Adsorption Data by the Intraparticle-Diffusion Models. *Chem. Eng. J.* **2010**, *163* (3), 256–263.
(122) Acevedo, B.; Barriocanal, C.; Lupul, I.; Gryglewicz, G. Properties and Performance of Mesoporous Activated Carbons from Scrap Tyres, Bituminous Wastes and Coal. *Fuel* **2015**, *151*, 83–90.
(123) Gupta, S. S.; Bhattacharyya, K. G. Kinetics of Adsorption of Metal Ions on Inorganic Materials: A Review. *Adv. Colloid Interface Sci.* **2011**, *162* (1–2), 39–58.
(124) Rudzinski, W.; Plazinski, W. On the Applicability of the Pseudo-Second Order Equation to Represent the Kinetics of Adsorption at Solid/Solution Interfaces: A Theoretical Analysis Based on the Statistical Rate Theory. *Adsorption* **2009**, *15* (2), 181.
(125) Tan, K. L.; Hameed, B. H. Insight into the Adsorption Kinetics Models for the Removal of Contaminants from Aqueous Solutions. *J. Taiwan Inst. Chem. Eng.* **2017**, *74*, 25–48.
(126) Zhang, R.; Zhang, J.; Zhang, X.; Dou, C.; Han, R. Adsorption of Congo Red from Aqueous Solutions Using Cationic Surfactant Modified Wheat Straw in Batch Mode: Kinetic and Equilibrium Study. *J. Taiwan Inst. Chem. Eng.* **2014**, *45* (5), 2578–2583.

(127) Ibrahim, Q.; Ali, I.; Kareem, S. Removal of Cetyldimethylbenzylammonium Chloride Surfactant from Aqueous Solution by Adsorption onto Mesoporous Silica. *Int. J. Sci. Res.* **2016**, *5*, 6–391.
(128) Sedeva, I. G.; Fornasiero, D.; Ralston, J.; Beattie, D. A. The Influence of Surface Hydrophobicity on Polyacrylamide Adsorption. *Langmuir* **2009**, *25* (8), 4514–4521.
(129) Wu, S.; Shi, L.; Garfield, L. B.; Tabor, R. F.; Striolo, A.; Grady, B. P. Influence of Surface Roughness on Cetyltrimethylammonium Bromide Adsorption from Aqueous Solution. *Langmuir* **2011**, *27* (10), 6091–6098.
(130) Llamas, S.; Guzmán, E.; Baghdadli, N.; Ortega, F.; Cazeneuve, C.; Rubio, R. G.; Luengo, G. S. Adsorption of Poly (Diallyldimethylammonium Chloride)—Sodium Methyl-Cocoyl-Taurate Complexes onto Solid Surfaces. *Colloids Surf. Physicochem. Eng. Asp.* **2016**, *505*, 150–157.
(131) Yu, Y.; Zhuang, Y.-Y.; Wang, Z.-H.; Qiu, M.-Q. Adsorption of Water-Soluble Dyes onto Modified Resin. *Chemosphere* **2004**, *54* (3), 425–430.
(132) Atkins, P.; De Paula, J. *Physical Chemistry for the Life Sciences*; Oxford University Press, USA, 2011.
(133) Liu, Y.; Liu, Y.-J. Biosorption Isotherms, Kinetics and Thermodynamics. *Sep. Purif. Technol.* **2008**, *61* (3), 229–242.
(134) Lima, E. C.; Hosseini-Bandegharaei, A.; Moreno-Piraján, J. C.; Anastopoulos, I. A Critical Review of the Estimation of the Thermodynamic Parameters on Adsorption Equilibria. Wrong Use of Equilibrium Constant in the Van't Hoof Equation for Calculation of Thermodynamic Parameters of Adsorption. *J. Mol. Liq.* **2019**, *273*, 425–434.
(135) Liu, Q.-S.; Zheng, T.; Wang, P.; Jiang, J.-P.; Li, N. Adsorption Isotherm, Kinetic and Mechanism Studies of Some Substituted Phenols on Activated Carbon Fibers. *Chem. Eng. J.* **2010**, *157* (2–3), 348–356.
(136) Macakova, L.; Blomberg, E.; Claesson, P. M. Effect of Adsorbed Layer Surface Roughness on the QCM-D Response: Focus on Trapped Water. *Langmuir* **2007**, *23* (24), 12436–12444.
(137) Sakai, K.; Koizumi, K.; Maeda, Y.; Endo, T.; Sasaki, S.; Abe, M.; Sakai, H. Adsolubilization-Induced Structural Change in Adsorbed Surfactant Aggregates: Equilibrium and Kinetics Monitored by AFM and QCM-D. *Colloids Surf. Physicochem. Eng. Asp.* **2017**, *520*, 231–238.
(138) Wanless, E. J.; Ducker, W. A. Organization of Sodium Dodecyl Sulfate at the Graphite− Solution Interface. *J. Phys. Chem.* **1996**, *100* (8), 3207–3214.
(139) Wangchareansak, T.; Craig, V. S.; Notley, S. M. Adsorption Isotherms and Structure of Cationic Surfactants Adsorbed on Mineral Oxide Surfaces Prepared by Atomic Layer Deposition. *Langmuir* **2013**, *29* (48), 14748–14755.
(140) Duval, F. P.; Zana, R.; Warr, G. G. Adsorbed Layer Structure of Cationic Gemini and Corresponding Monomeric Surfactants on Mica. *Langmuir* **2006**, *22* (3), 1143–1149.
(141) Inoue, S.; Uchihashi, T.; Yamamoto, D.; Ando, T. Direct Observation of Surfactant Aggregate Behavior on a Mica Surface Using High-Speed Atomic Force Microscopy. *Chem. Commun.* **2011**, *47* (17), 4974–4976.
(142) Yang, H.; Duan, H.; Wu, X.; Wang, M.; Chen, T.; Liu, F.; Huang, S.; Zhang, W.; Chen, G.; Yu, D. Self-Assembly Behavior of Ultrahighly Charged Amphiphilic Polyelectrolyte on Solid Surfaces. *Langmuir* **2016**, *32* (44), 11485–11491.
(143) Rodenhausen, K. B.; Guericke, M.; Sarkar, A.; Hofmann, T.; Ianno, N.; Schubert, M.; Tiwald, T. E.; Solinsky, M.; Wagner, M. Micelle-Assisted Bilayer Formation of Cetyltrimethylammonium Bromide Thin Films Studied with Combinatorial Spectroscopic Ellipsometry and Quartz Crystal Microbalance Techniques. *Thin Solid Films* **2011**, *519* (9), 2821–2824.
(144) Fang, J.; Du, X.; Ma, Q.; Zhu, D.-M. Specific Responses of Surface Plasmon Resonance and Quartz Crystal Microbalance Techniques to the Mass of Adsorbates at Solid-Liquid Interfaces. *Sens. Actuators B Chem.* **2018**, *277*, 241–249.
(145) Fragneto, G.; Thomas, R. K.; Rennie, A. R.; Penfold, J. Neutron Reflection from Hexadecyltrimethylammonium Bromide Adsorbed on Smooth and Rough Silicon Surfaces. *Langmuir* **1996**, *12* (25), 6036–6043.
(146) Li, Z. X.; Dong, C. C.; Thomas, R. K. Neutron Reflectivity Studies of the Surface Excess of Gemini Surfactants at the Air− Water Interface. *Langmuir* **1999**, *15* (13), 4392–4396.

(147) Penfold, J.; Staples, E.; Tucker, I.; Thomas, R. K. Adsorption of Mixed Anionic and Nonionic Surfactants at the Hydrophilic Silicon Surface. *Langmuir* **2002**, *18* (15), 5755–5760.
(148) Wolanin, J.; Barré, L.; Dalmazzone, C.; Frot, D.; Jestin, J.; Perrot, H.; Bauer, D. Insight into Kinetics and Mechanisms of AOT Vesicle Adsorption on Silica in Unfavorable Conditions. *Langmuir* **2020**, *36* (8), 1937–1949.
(149) Garcia-Olvera, G.; Reilly, T.; Lehmann, T. E.; Zhang, L.; Alvarado, V. Surfactant Behavior Analysis in Enhanced Oil Recovery Blends Using One-Dimensional Proton Nuclear Magnetic Resonance. *Energy Fuels* **2016**, *30* (1), 63–71.
(150) Tyrode, E.; Rutland, M. W.; Bain, C. D. Adsorption of CTAB on Hydrophilic Silica Studied by Linear and Nonlinear Optical Spectroscopy. *J. Am. Chem. Soc.* **2008**, *130* (51), 17434–17445.
(151) Woods, D. A.; Bain, C. D. Total Internal Reflection Raman Spectroscopy. *Analyst* **2012**, *137* (1), 35–48.
(152) Schrödle, S.; Richmond, G. L. Equilibrium and Non-Equilibrium Kinetics of Self-Assembled Surfactant Monolayers: A Vibrational Sum-Frequency Study of Dodecanoate at the Fluorite−Water Interface. *J. Am. Chem. Soc.* **2008**, *130* (15), 5072–5085.
(153) Tummala, N. R.; Shi, L.; Striolo, A. Molecular Dynamics Simulations of Surfactants at the Silica–Water Interface: Anionic vs Nonionic Headgroups. *J. Colloid Interface Sci.* **2011**, *362* (1), 135–143.
(154) Liu, Z.; Yu, J.-G.; O'Rear, E. A.; Striolo, A. Aqueous Dual-Tailed Surfactants Simulated on the Alumina Surface. *J. Phys. Chem. B* **2014**, *118* (32), 9695–9707.
(155) Jiménez-Ángeles, F.; Khoshnood, A.; Firoozabadi, A. Molecular Dynamics Simulation of the Adsorption and Aggregation of Ionic Surfactants at Liquid–Solid Interfaces. *J. Phys. Chem. C* **2017**, *121* (46), 25908–25920.
(156) Sammalkorpi, M.; Panagiotopoulos, A. Z.; Haataja, M. Surfactant and Hydrocarbon Aggregates on Defective Graphite Surface: Structure and Dynamics. *J. Phys. Chem. B* **2008**, *112* (41), 12954–12961.
(157) Suttipong, M.; Grady, B. P.; Striolo, A. Surfactant Aggregates Templated by Lateral Confinement. *J. Phys. Chem. B* **2015**, *119* (17), 5467–5474.
(158) Suttipong, M.; Grady, B. P.; Striolo, A. Surfactants Adsorption on Crossing Stripes and Steps. *Soft Matter* **2017**, *13* (4), 862–874.
(159) Xu, L.; Wu, H.; Dong, F.; Wang, L.; Wang, Z.; Xiao, J. Flotation and Adsorption of Mixed Cationic/Anionic Collectors on Muscovite Mica. *Miner. Eng.* **2013**, *41*, 41–45.
(160) Li, X.; Xue, Q.; Zhu, L.; Jin, Y.; Wu, T.; Guo, Q.; Zheng, H.; Lu, S. How to Select an Optimal Surfactant Molecule to Speed up the Oil-Detachment from Solid Surface: A Computational Simulation. *Chem. Eng. Sci.* **2016**, *147*, 47–53.
(161) Barnes, J. R.; Smit, J.; Smit, J.; Shpakoff, G.; Raney, K. H.; Puerto, M. Development of Surfactants for Chemical Flooding at Difficult Reservoir Conditions. In *SPE Symposium on Improved Oil Recovery*; Society of Petroleum Engineers, 2008.
(162) Seethepalli, A.; Adibhatla, B.; Mohanty, K. K. Wettability Alteration during Surfactant Flooding of Carbonate Reservoirs. In *SPE/DOE symposium on improved oil recovery*; Society of Petroleum Engineers, 2004.
(163) Amirmoshiri, M.; Zhang, L.; Puerto, M. C.; Tewari, R. D.; Bahrim, R. Z. B. K.; Farajzadeh, R.; Hirasaki, G. J.; Biswal, S. L. Role of Wettability on the Adsorption of an Anionic Surfactant on Sandstone Cores. *Langmuir* **2020**, *36* (36), 10725–10738.
(164) Southwick, J. G.; van den Pol, E.; van Rijn, C. H.; van Batenburg, D. W.; Boersma, D.; Svec, Y.; Anis Mastan, A.; Shahin, G.; Raney, K. Ammonia as Alkali for Alkaline/Surfactant/Polymer Floods. *Spe J.* **2016**, *21* (01), 10–21.
(165) Zeng, T.; Kim, K. T.; Werth, C. J.; Katz, L. E.; Mohanty, K. K. Surfactant Adsorption on Shale Samples: Experiments and an Additive Model. *Energy Fuels* **2020**.
(166) Kumar, A.; Mandal, A. Synthesis and Physiochemical Characterization of Zwitterionic Surfactant for Application in Enhanced Oil Recovery. *J. Mol. Liq.* **2017**, *243*, 61–71.
(167) Druetta, P.; Raffa, P.; Picchioni, F. Chemical Enhanced Oil Recovery and the Role of Chemical Product Design. *Appl. Energy* **2019**, *252*, 113480.

(168) Lv, W.; Bazin, B.; Ma, D.; Liu, Q.; Han, D.; Wu, K. Static and Dynamic Adsorption of Anionic and Amphoteric Surfactants with and without the Presence of Alkali. *J. Pet. Sci. Eng.* **2011**, *77* (2), 209–218.
(169) Wang, W.; Kwak, J. C. Adsorption at the Alumina–Water Interface from Mixed Surfactant Solutions. *Colloids Surf. Physicochem. Eng. Asp.* **1999**, *156* (1–3), 95–110.
(170) Muherei, M. A.; Junin, R.; Merdhah, A. B. B. Adsorption of Sodium Dodecyl Sulfate, Triton X100 and Their Mixtures to Shale and Sandstone: A Comparative Study. *J. Pet. Sci. Eng.* **2009**, *67* (3–4), 149–154.
(171) Yang, K.; Zhu, L.; Zhao, B. Minimizing Losses of Nonionic and Anionic Surfactants to a Montmorillonite Saturated with Calcium Using Their Mixtures. *J. Colloid Interface Sci.* **2005**, *291* (1), 59–66.
(172) Zhang, Y.; Zhao, Y.; Zhu, Y.; Wu, H.; Wang, H.; Lu, W. Adsorption of Mixed Cationic-Nonionic Surfactant and Its Effect on Bentonite Structure. *J. Environ. Sci.* **2012**, *24* (8), 1525–1532.
(173) Zhou, Q.; Somasundaran, P. Synergistic Adsorption of Mixtures of Cationic Gemini and Nonionic Sugar-Based Surfactant on Silica. *J. Colloid Interface Sci.* **2009**, *331* (2), 288–294.
(174) Hou, B.; Jia, R.; Fu, M.; Wang, Y.; Bai, Y.; Huang, Y. Wettability Alteration of an Oil-Wet Sandstone Surface by Synergistic Adsorption/Desorption of Cationic/Nonionic Surfactant Mixtures. *Energy Fuels* **2018**, *32* (12), 12462–12468.
(175) Li, Y.; Zhang, W.; Kong, B.; Puerto, M.; Bao, X.; Sha, O.; Shen, Z.; Yang, Y.; Liu, Y.; Gu, S. Mixtures of Anionic/Cationic Surfactants: A New Approach for Enhanced Oil Recovery in Low-Salinity, High-Temperature Sandstone Reservoir. *SPE J.* **2016**, *21* (04), 1,164-1,177.
(176) He, K.; Xu, L. Unique Mixtures of Anionic/Cationic Surfactants: A New Approach to Enhance Surfactant Performance in Liquids-Rich Shale Reservoirs. In *SPE International Conference on Oilfield Chemistry*; Society of Petroleum Engineers, 2017.
(177) Wu, Y. al; Iglauer, S.; Shuler, P.; Tang, Y.; Goddard III, W. A. Branched Alkyl Alcohol Propoxylated Sulfate Surfactants for Improved Oil Recovery. *Tenside Surfactants Deterg.* **2010**, *47* (3), 152–161.
(178) Tiberg, F.; Joensson, B.; Tang, J.; Lindman, B. Ellipsometry Studies of the Self-Assembly of Nonionic Surfactants at the Silica-Water Interface: Equilibrium Aspects. *Langmuir* **1994**, *10* (7), 2294–2300.
(179) Levitt, D. B.; Dufour, S.; Pope, G.; Morel, D.; Gauer, P. Design of an ASP Flood in a High-Temperature, High-Salinity, Low-Permeability Carbonate. In *IPTC 2012: International Petroleum Technology Conference*; European Association of Geoscientists & Engineers, 2012; p cp-280-00209.
(180) Chen, Y.; Xu, G. Improvement of Ca2+-Tolerance by the Introduction of EO Groups for the Anionic Surfactants: Molecular Dynamics Simulation. *Colloids Surf. Physicochem. Eng. Asp.* **2013**, *424*, 26–32.
(181) Salager, J.-L.; Antón, R. E.; Sabatini, D. A.; Harwell, J. H.; Acosta, E. J.; Tolosa, L. I. Enhancing Solubilization in Microemulsions—State of the Art and Current Trends. *J. Surfactants Deterg.* **2005**, *8* (1), 3–21.
(182) Kathel, P.; Mohanty, K. K. EOR in Tight Oil Reservoirs through Wettability Alteration. In *SPE Annual Technical Conference and Exhibition*; Society of Petroleum Engineers, 2013.
(183) Sunwoo, C. K.; Wade, W. H. Optimal Surfactant Structures for Cosurfactant-Free Microemulston Systems I. C16 and C14 Guerbet Alcohol Hydrophobes. *J. Dispers. Sci. Technol.* **1992**, *13* (5), 491–514.
(184) Zhao, T.; Feng, N.; Zhao, Y.; Zhang, G. Adsorption Behavior and Application Performance of Branched Aliphatic Alcohol Polyoxyethylene Ether Phosphate. *Colloids Surf. Physicochem. Eng. Asp.* **2020**, *606*, 125482.
(185) Somasundaran, P.; Middleton, R.; Viswanathan, K. V. Relationship between Surfactant Structure and Adsorption. *Struct. Relatsh. Surfactants* **1984**, *253*, 269.
(186) Wilson, D.; Poindexter, L.; Nguyen, T. Role of Surfactant Structures on Surfactant-Rock Adsorption in Various Rock Types. In *SPE International Conference on Oilfield Chemistry*; Society of Petroleum Engineers, 2019.

(187) Apaydin, O. G.; Kovscek, A. R. Surfactant Concentration and End Effects on Foam Flow in Porous Media. *Transp. Porous Media* **2001**, *43* (3), 511–536.
(188) Ma, K.; Cui, L.; Dong, Y.; Wang, T.; Da, C.; Hirasaki, G. J.; Biswal, S. L. Adsorption of Cationic and Anionic Surfactants on Natural and Synthetic Carbonate Materials. *J. Colloid Interface Sci.* **2013**, *408*, 164–172.
(189) Tagavifar, M.; Jang, S. H.; Sharma, H.; Wang, D.; Chang, L. Y.; Mohanty, K.; Pope, G. A. Effect of PH on Adsorption of Anionic Surfactants on Limestone: Experimental Study and Surface Complexation Modeling. *Colloids Surf. Physicochem. Eng. Asp.* **2018**, *538*, 549–558.
(190) Karaguzel, C.; Xu, Z. Effect of PH on Adsorption and Desorption of Hexadecyl Trimethyl Ammonium Bromide from Silicate Surface. *Physicochem. Probl. Miner. Process.* **2017**, *53*.
(191) Liu, Z. L.; Rios-Carvajal, T.; Andersson, M. P.; Ceccato, M.; Stipp, S. L. S.; Hassenkam, T. Insights into the Pore-Scale Mechanism for the Low-Salinity Effect: Implications for Enhanced Oil Recovery. *Energy Fuels* **2018**, *32* (12), 12081–12090.
(192) Liu, Z.; Rios-Carvajal, T.; Andersson, M. P.; Stipp, S.; Hassenkam, T. Ion Effects on Molecular Interaction between Graphene Oxide and Organic Molecules. *Environ. Sci. Nano* **2019**.
(193) Gerold, C. T.; Henry, C. S. Observation of Dynamic Surfactant Adsorption Facilitated by Divalent Cation Bridging. *Langmuir* **2018**, *34* (4), 1550–1556.
(194) Wanless, E. J.; Ducker, W. A. Weak Influence of Divalent Ions on Anionic Surfactant Surface-Aggregation. *Langmuir* **1997**, *13* (6), 1463–1474.
(195) Solongo, S. K.; Gomez-Flores, A.; You, J.; Choi, S.; Heyes, G. W.; Ilyas, S.; Lee, J.; Kim, H. Cationic Collector Conformations on an Oxide Mineral Interface: Roles of PH, Ionic Strength, and Ion Valence. *Miner. Eng.* **2020**, *150*, 106277.
(196) Nevskaia, D. M.; Guerrero-Ruız, A.; López-González, J. de D. Adsorption of Polyoxyethylenic Nonionic and Anionic Surfactants from Aqueous Solution: Effects Induced by the Addition of NaCl and CaCl2. *J. Colloid Interface Sci.* **1998**, *205* (1), 97–105.
(197) Al-Hashim, H. S.; Celik, M. S.; Oskay, M. M.; Al-Yousef, H. Y. Adsorption and Precipitation Behaviour of Petroleum Sulfonates from Saudi Arabian Limestone. *J. Pet. Sci. Eng.* **1988**, *1* (4), 335–344.
(198) AlQuraishi, A. A.; AlHussinan, S. N.; AlYami, H. Q. Efficiency and Recovery Mechanisms of Low Salinity Water Flooding in Sandstone and Carbonate Reservoirs. In *Offshore Mediterranean Conference and Exhibition*; Offshore Mediterranean Conference, 2015.
(199) Azam, M. R.; Tan, I. M.; Ismail, L.; Mushtaq, M.; Nadeem, M.; Sagir, M. Static Adsorption of Anionic Surfactant onto Crushed Berea Sandstone. *J. Pet. Explor. Prod. Technol.* **2013**, *3* (3), 195–201.
(200) Johannessen, A. M.; Spildo, K. Enhanced Oil Recovery (EOR) by Combining Surfactant with Low Salinity Injection. *Energy Fuels* **2013**, *27* (10), 5738–5749.
(201) Nourani, M.; Tichelkamp, T.; Gaweł, B.; Øye, G. Desorption of Crude Oil Components from Silica and Aluminosilicate Surfaces upon Exposure to Aqueous Low Salinity and Surfactant Solutions. *Fuel* **2016**, *180*, 1–8.
(202) Kwok, W.; Nasr-El-Din, H. A.; Hayes, R. E. Propagation of an Anionic Surfactant in Radial Sandstone Cores. *J. Can. Pet. Technol.* **1993**, *32* (06).
(203) Thibaut, A.; Misselyn-Bauduin, A.-M.; Grandjean, J.; Broze, G.; Jérôme, R. Adsorption of an Aqueous Mixture of Surfactants on Silica. *Langmuir* **2000**, *16* (24), 9192–9198.
(204) Wang, L.; Siretanu, I.; Duits, M. H.; Stuart, M. A. C.; Mugele, F. Ion Effects in the Adsorption of Carboxylate on Oxide Surfaces, Studied with Quartz Crystal Microbalance. *Colloids Surf. Physicochem. Eng. Asp.* **2016**, *494*, 30–38.
(205) Wang, F. H. L. Effects of Reservoir Anaerobic, Reducing Conditions on Surfactant Retention in Chemical Flooding. *SPE Reserv. Eng.* **1993**, *8* (02), 108–116.
(206) Tombácz, E.; Szekeres, M. Surface Charge Heterogeneity of Kaolinite in Aqueous Suspension in Comparison with Montmorillonite. *Appl. Clay Sci.* **2006**, *34* (1–4), 105–124.
(207) Torn, L. H.; De Keizer, A.; Koopal, L. K.; Lyklema, J. Mixed Adsorption of Poly (Vinylpyrrolidone) and Sodium Dodecylbenzenesulfonate on Kaolinite. *J. Colloid Interface Sci.* **2003**, *260* (1), 1–8.

(208) Tang, G.-Q.; Morrow, N. R. Influence of Brine Composition and Fines Migration on Crude Oil/Brine/Rock Interactions and Oil Recovery. *J. Pet. Sci. Eng.* **1999**, *24* (2–4), 99–111.
(209) Figdore, P. E. Adsorption of Surfactants on Kaolinite: NaCl versus CaCl2 Salt Effects. *J. Colloid Interface Sci.* **1982**, *87* (2), 500–517.
(210) Saha, R.; Uppaluri, R. V.; Tiwari, P. Effect of Mineralogy on the Adsorption Characteristics of Surfactant—Reservoir Rock System. *Colloids Surf. Physicochem. Eng. Asp.* **2017**, *531*, 121–132.
(211) Akbar, M.; Vissapragada, B.; Alghamdi, A. H.; Allen, D.; Herron, M.; Carnegie, A.; Dutta, D.; Olesen, J.-R.; Chourasiya, R. D.; Logan, D. A Snapshot of Carbonate Reservoir Evaluation. *Oilfield Rev.* **2000**, *12* (4), 20–21.
(212) Kalwar, S. A.; Elraies, K. A.; Memon, M. K.; Kumar, S.; Abbas, G.; Mithani, A. H. A New Approach to ASP Flooding in High Saline and Hard Carbonate Reservoirs. In *International Petroleum Technology Conference*; International Petroleum Technology Conference, 2014.
(213) Ahmadall, T.; Gonzalez, M. V.; Harwell, J. H.; Scamehorn, J. F. Reducing Surfactant Adsorption in Carbonate Reservoirs. *SPE Reserv. Eng.* **1993**, *8* (02), 117–122.
(214) Sánchez-Martín, M. J.; Dorado, M. C.; Del Hoyo, C.; Rodríguez-Cruz, M. S. Influence of Clay Mineral Structure and Surfactant Nature on the Adsorption Capacity of Surfactants by Clays. *J. Hazard. Mater.* **2008**, *150* (1), 115–123.
(215) Gao, Z.; Sun, W.; Hu, Y. New Insights into the Dodecylamine Adsorption on Scheelite and Calcite: An Adsorption Model. *Miner. Eng.* **2015**, *79*, 54–61.
(216) Grigg, R. B.; Bai, B. Sorption of Surfactant Used in CO2 Flooding onto Five Minerals and Three Porous Media. In *SPE International Symposium on Oilfield Chemistry*; Society of Petroleum Engineers, 2005.
(217) Mirchi*, V.; Saraji, S.; Goual, L.; Piri, M. Experimental Investigation of Surfactant Flooding in Shale Oil Reservoirs: Dynamic Interfacial Tension, Adsorption, and Wettability. In *Unconventional Resources Technology Conference, Denver, Colorado, 25-27 August 2014*; Society of Exploration Geophysicists, American Association of Petroleum …, 2014; pp 1619–1624.
(218) Zhang, J.; Wang, D.; Olatunji, K. Surfactant Adsorption Investigation in Ultra-Lower Permeable Rocks. In *SPE Low Perm Symposium*; Society of Petroleum Engineers, 2016.
(219) Alvarez, J. O.; Saputra, I. W. R.; Schechter, D. S. Potential of Improving Oil Recovery with Surfactant Additives to Completion Fluids for the Bakken. *Energy Fuels* **2017**, *31* (6), 5982–5994.
(220) Pavan, P. C.; Crepaldi, E. L.; Gomes, G. de A.; Valim, J. B. Adsorption of Sodium Dodecylsulfate on a Hydrotalcite-like Compound. Effect of Temperature, PH and Ionic Strength. *Colloids Surf. Physicochem. Eng. Asp.* **1999**, *154* (3), 399–410.
(221) Yekeen, N.; Manan, M. A.; Idris, A. K.; Samin, A. M. Influence of Surfactant and Electrolyte Concentrations on Surfactant Adsorption and Foaming Characteristics. *J. Pet. Sci. Eng.* **2017**, *149*, 612–622.
(222) Mohajeri, E.; Noudeh, G. D. Effect of Temperature on the Critical Micelle Concentration and Micellization Thermodynamic of Nonionic Surfactants: Polyoxyethylene Sorbitan Fatty Acid Esters. *J. Chem.* **2012**, *9* (4), 2268–2274.
(223) Negin, C.; Ali, S.; Xie, Q. Most Common Surfactants Employed in Chemical Enhanced Oil Recovery. *Petroleum* **2017**, *3* (2), 197–211.
(224) Corkill, J. M.; Goodman, J. F.; Tate, J. R. Adsorption of Non-Ionic Surface-Active Agents at the Graphon/Solution Interface. *Trans. Faraday Soc.* **1966**, *62*, 979–986.
(225) Ziegler, V. M.; Handy, L. L. Effect of Temperature on Surfactant Adsorption in Porous Media. *Soc. Pet. Eng. J.* **1981**, *21* (02), 218–228.
(226) Zhao, G.; Khin, C. C.; Chen, S. B.; Chen, B.-H. Nonionic Surfactant and Temperature Effects on the Viscosity of Hydrophobically Modified Hydroxyethyl Cellulose Solutions. *J. Phys. Chem. B* **2005**, *109* (29), 14198–14204.
(227) Bataweel, M. A.; Nasr-El-Din, H. A. ASP vs. SP Flooding in High Salinity/Hardness and Temperature in Sandstone Cores. In *SPE EOR Conference at Oil and Gas West Asia*; Society of Petroleum Engineers, 2012.

(228) Lin, W.; Li, X.; Yang, Z.; WANG, J.; YOU, Q.; ZHANG, Y.; HE, Y. A Laboratory Study of Surfactant Flooding System for Tertiary Recovery in High-Temperature and High-Salinity Reservoirs. *J. Residuals Sci. Technol.* **2017**, *14*.
(229) Puerto, M.; Hirasaki, G. J.; Miller, C. A.; Barnes, J. R. Surfactant Systems for EOR in High-Temperature, High-Salinity Environments. *SPE J.* **2012**, *17* (01), 11–19.
(230) Austad, T.; Strand, S. Chemical Flooding of Oil Reservoirs 4. Effects of Temperature and Pressure on the Middle Phase Solubilization Parameters Close to Optimum Flood Conditions. *Colloids Surf. Physicochem. Eng. Asp.* **1996**, *108* (2–3), 243–252.
(231) Roshanfekr, M.; Johns, R. T.; Pope, G.; Britton, L.; Linnemeyer, H.; Britton, C.; Vyssotski, A. Simulation of the Effect of Pressure and Solution Gas on Oil Recovery from Surfactant/Polymer Floods. *SPE J.* **2012**, *17* (03), 705–716.
(232) Flaaten, A. K.; Nguyen, Q. P.; Zhang, J.; Mohammadi, H.; Pope, G. A. Alkaline/Surfactant/Polymer Chemical Flooding without the Need for Soft Water. *SPE J.* **2010**, *15* (01), 184–196.
(233) Guo, H.; Li, Y.; Wang, F.; Gu, Y. Comparison of Strong-Alkali and Weak-Alkali ASP-Flooding Field Tests in Daqing Oil Field. *SPE Prod. Oper.* **2018**, *33* (02), 353–362.
(234) Deng, X.; Kamal, M. S.; Patil, S.; hussain, syed; Zhou, X. A Review on Wettability Alteration in Carbonate Rocks: Wettability Modifiers. *Energy Fuels* **2019**.
(235) Sheng, J. J. A Comprehensive Review of Alkaline–Surfactant–Polymer (ASP) Flooding. *Asia-Pacific J. Chem. Eng.* **2014**, *9* (4), 471–489.
(236) Zhang, D.; Liu, S.; Yan, W.; Puerto, M.; Hirasaki, G. J.; Miller, C. A. Favorable Attributes of Alkali-Surfactant-Polymer Flooding. In *SPE/DOE Symposium on Improved Oil Recovery*; Society of Petroleum Engineers, 2006.
(237) Liu, S.; Zhang, D.; Yan, W.; Puerto, M.; Hirasaki, G. J.; Miller, C. A. Favorable Attributes of Alkaline-Surfactant-Polymer Flooding. *SPE J.* **2008**, *13* (01), 5–16.
(238) Southwick, J. G. Solubility of Silica in Alkaline Solutions: Implications for Alkaline Flooding. *Soc. Pet. Eng. J.* **1985**, *25* (06), 857–864.
(239) Zhong, H.; Yang, T.; Yin, H.; Fu, C.; Lu, J. The Role of Chemicals Loss in Sandstone Formation in ASP Flooding Enhanced Oil Recovery. In *SPE Annual Technical Conference and Exhibition*; Society of Petroleum Engineers, 2018.
(240) Wang, D.; Maubert, M.; Pope, G. A.; Liyanage, P. J.; Jang, S. H.; Upamali, K. A.; Chang, L.; Tagavifar, M.; Sharma, H.; Ren, G. Reduction of Surfactant Retention in Limestones Using Sodium Hydroxide. *SPE J.* **2019**, *24* (01), 92–115.
(241) Maubert, M.; Jith Liyanage, P.; Pope, G.; Upamali, N.; Chang, L.; Ren, G.; Mateen, K.; Ma, K.; Bourdarot, G.; Morel, D. ASP Experiments in Indiana Limestone Using NaOH to Reduce Surfactant Retention. In *SPE Improved Oil Recovery Conference*; Society of Petroleum Engineers, 2018.
(242) Tagavifar, M.; Sharma, H.; Wang, D.; Jang, S. H.; Pope, G. Alkaline/Surfactant/Polymer Flooding with Sodium Hydroxide in Indiana Limestone: Analysis of Water/Rock Interactions and Surfactant Adsorption. *SPE J.* **2018**, *23* (06), 2,279-2,301.
(243) Zhang, J.; Nguyen, Q. P.; Flaaten, A.; Pope, G. A. Mechanisms of Enhanced Natural Imbibition with Novel Chemicals. *SPE Reserv. Eval. Eng.* **2009**, *12* (06), 912–920.
(244) Unomah, M. O. Chemical Enhanced Oil Recovery Utilizing Alternative Alkalis. **2013**.
(245) Berger, P. D.; Lee, C. H. Improved ASP Process Using Organic Alkali. In *SPE/DOE symposium on improved oil recovery*; Society of Petroleum Engineers, 2006.
(246) Zhao, F.; Ma, Y.; Hou, J.; Tang, J.; Xie, D. Feasibility and Mechanism of Compound Flooding of High-Temperature Reservoirs Using Organic Alkali. *J. Pet. Sci. Eng.* **2015**, *135*, 88–100.
(247) Hong, S. A.; Bae, J. H.; Lewis, G. R. An Evaluation of Lignosulfonate as a Sacrificial Adsorbate in Surfactant Flooding. *SPE Reserv. Eng.* **1987**, *2* (01), 17–27.
(248) Tsau, J.-S.; Syahputra, A. E.; Grigg, R. B. Economic Evaluation of Surfactant Adsorption in Co2 Foam Application. In *SPE/DOE Improved Oil Recovery Symposium*; Society of Petroleum Engineers, 2000.
(249) Shamsijazeyi, H.; Hirasaki, G.; Verduzco, R. Sacrificial Agent for Reducing Adsorption of Anionic Surfactants. In *SPE International Symposium on Oilfield Chemistry*; Society of Petroleum Engineers, 2013.

(250) ShamsiJazeyi, H.; Verduzco, R.; Hirasaki, G. J. Reducing Adsorption of Anionic Surfactant for Enhanced Oil Recovery: Part I. Competitive Adsorption Mechanism. *Colloids Surf. Physicochem. Eng. Asp.* **2014**, *453*, 162–167.
(251) Esumi, K.; Iitaka, M.; Koide, Y. Simultaneous Adsorption of Poly (Ethylene Oxide) and Cationic Surfactant at the Silica/Water Interface. *J. Colloid Interface Sci.* **1998**, *208* (1), 178–182.
(252) Budhathoki, M.; Barnee, S. H. R.; Shiau, B.-J.; Harwell, J. H. Improved Oil Recovery by Reducing Surfactant Adsorption with Polyelectrolyte in High Saline Brine. *Colloids Surf. Physicochem. Eng. Asp.* **2016**, *498*, 66–73.
(253) Weston, J. S.; Harwell, J. H.; Shiau, B. J.; Kabir, M. Disrupting Admicelle Formation and Preventing Surfactant Adsorption on Metal Oxide Surfaces Using Sacrificial Polyelectrolytes. *Langmuir* **2014**, *30* (22), 6384–6388.
(254) Wang, J.; Han, M.; Fuseni, A. B.; Cao, D. Surfactant Adsorption in Surfactant-Polymer Flooding for Carbonate Reservoirs. In *SPE Middle East Oil & Gas Show and Conference*; Society of Petroleum Engineers, 2015.
(255) Daoshan, L.; Shouliang, L.; Yi, L.; Demin, W. The Effect of Biosurfactant on the Interfacial Tension and Adsorption Loss of Surfactant in ASP Flooding. *Colloids Surf. Physicochem. Eng. Asp.* **2004**, *244* (1–3), 53–60.
(256) Liu, Z.; Hedayati, P.; Ghatkesar, M. K.; Sun, W.; Onay, H.; Groenendijk, D.; van Wunnik, J.; Sudhölter, E. J. Reducing Anionic Surfactant Adsorption Using Polyacrylate as Sacrificial Agent Investigated by QCM-D. *J. Colloid Interface Sci.* **2021**, *585*, 1–11.
(257) Tumba, J.; Agi, A.; Gbadamosi, A.; Junin, R.; Abbas, A.; Rajaei, K.; Gbonhinbor, J. Lignin As a Potential Additive For Minimizing Surfactant Adsorption On Clay Minerals In Different Electrolyte Concentration. In *SPE Nigeria Annual International Conference and Exhibition*; Society of Petroleum Engineers, 2019.
(258) He, K.; Yue, Z.; Fan, C.; Xu, L. Minimizing Surfactant Adsorption Using Polyelectrolyte Based Sacrificial Agent: A Way to Optimize Surfactant Performance in Unconventional Formations. In *SPE international symposium on oilfield chemistry*; Society of Petroleum Engineers, 2015.
(259) Velegol, S. B.; Tilton, R. D. Specific Counterion Effects on the Competitive Co-Adsorption of Polyelectrolytes and Ionic Surfactants. *J. Colloid Interface Sci.* **2002**, *249* (2), 282–289.
(260) Fredd, C. N.; Fogler, H. S. Chelating Agents as Effective Matrix Stimulation Fluids for Carbonate Formations. In *International symposium on oilfield chemistry*; Society of Petroleum Engineers, 1997.
(261) Yang, C.; Bazin, B.; Labrid, T.; Liu, Y. Reduction Of Surfactant Retention With Polyphosphates In Surfactants Flooding Process. In *International Meeting on Petroleum Engineering*; Society of Petroleum Engineers, 1988.
(262) Mahmoud, A. A.; Al-Hashim, H. Insight into the Mechanism for Oil Recovery Using EDTA Chelating Agent Solutions from Clayey Sandstone Rocks. *J. Pet. Sci. Eng.* **2018**, *161*, 625–635.
(263) Levitt, D.; Bourrel, M. Adsorption of EOR Chemicals under Laboratory and Reservoir Conditions, Part III: Chemical Treatment Methods. In *SPE Improved Oil Recovery Conference*; Society of Petroleum Engineers, 2016.
(264) Franco-Aguirre, M.; Zabala, R. D.; Lopera, S. H.; Franco, C. A.; Cortés, F. B. Ca-DTPMP Nanoparticles-Based Nanofluids for the Inhibition and Remediation of Formation Damage Due to CaCO3 Scaling in Tight Gas-Condensate Reservoirs. *J. Pet. Sci. Eng.* **2018**, *169*, 636–645.
(265) Wu, Y.; Chen, W.; Dai, C.; Huang, Y.; Li, H.; Zhao, M.; He, L.; Jiao, B. Reducing Surfactant Adsorption on Rock by Silica Nanoparticles for Enhanced Oil Recovery. *J. Pet. Sci. Eng.* **2017**, *153*, 283–287.
(266) Suresh, R.; Kuznetsov, O.; Agrawal, D.; Darugar, Q.; Khabashesku, V. Reduction of Surfactant Adsorption in Porous Media Using Silica Nanoparticles. In *Offshore technology conference*; Offshore Technology Conference, 2018.
(267) Yekeen, N.; Manan, M. A.; Idris, A. K.; Samin, A. M.; Risal, A. R. Experimental Investigation of Minimization in Surfactant Adsorption and Improvement in Surfactant-Foam Stability in Presence of Silicon Dioxide and Aluminum Oxide Nanoparticles. *J. Pet. Sci. Eng.* **2017**, *159*, 115–134.

(268) Zargartalebi, M.; Kharrat, R.; Barati, N. Enhancement of Surfactant Flooding Performance by the Use of Silica Nanoparticles. *Fuel* **2015**, *143*, 21–27.
(269) Ahmadi, M. A.; Shadizadeh, S. R. Induced Effect of Adding Nano Silica on Adsorption of a Natural Surfactant onto Sandstone Rock: Experimental and Theoretical Study. *J. Pet. Sci. Eng.* **2013**, *112*, 239–247.
(270) Zhong, X.; Li, C.; Pu, H.; Zhou, Y.; Zhao, J. X. Increased Nonionic Surfactant Efficiency in Oil Recovery by Integrating with Hydrophilic Silica Nanoparticle. *Energy Fuels* **2019**, *33* (9), 8522–8529.
(271) Zhong, X.; Li, C.; Li, Y.; Pu, H.; Zhou, Y.; Zhao, J. X. Enhanced Oil Recovery in High Salinity and Elevated Temperature Conditions with a Zwitterionic Surfactant and Silica Nanoparticles Acting in Synergy. *Energy Fuels* **2020**, *34* (3), 2893–2902.
(272) Betancur, S.; Carrasco-Marín, F.; Franco, C. A.; Cortés, F. B. Development of Composite Materials Based on the Interaction between Nanoparticles and Surfactants for Application in Chemical Enhanced Oil Recovery. *Ind. Eng. Chem. Res.* **2018**, *57* (37), 12367–12377.
(273) Betancur, S.; Carrasco-Marín, F.; Pérez-Cadenas, A. F.; Franco, C. A.; Jiménez, J.; Manrique, E. J.; Quintero, H.; Cortés, F. B. Effect of Magnetic Iron Core–Carbon Shell Nanoparticles in Chemical Enhanced Oil Recovery for Ultralow Interfacial Tension Region. *Energy Fuels* **2019**, *33* (5), 4158–4168.
(274) Gizzatov, A.; Mashat, A.; Kosynkin, D.; Alhazza, N.; Kmetz, A.; Eichmann, S. L.; Abdel-Fattah, A. I. Nanofluid of Petroleum Sulfonate Nanocapsules for Enhanced Oil Recovery in High-Temperature and High-Salinity Reservoirs. *Energy Fuels* **2019**, *33* (11), 11567–11573.
(275) Ulbrich, K.; Hola, K.; Subr, V.; Bakandritsos, A.; Tucek, J.; Zboril, R. Targeted Drug Delivery with Polymers and Magnetic Nanoparticles: Covalent and Noncovalent Approaches, Release Control, and Clinical Studies. *Chem. Rev.* **2016**, *116* (9), 5338–5431.
(276) Neves Libório De Avila, J.; Louise Grecco Cavalcanti De Araujo, L.; Drexler, S.; de Almeida Rodrigues, J.; Sandra Veiga Nascimento, R. Polystyrene Nanoparticles as Surfactant Carriers for Enhanced Oil Recovery. *J. Appl. Polym. Sci.* **2016**, *133* (32).
(277) PC Caplan, S.; BG Silva, T.; DS Franscisco, A.; R Lachter, E.; SV Nascimento, R. Sulfonated Polystyrene Nanoparticles as Oleic Acid Diethanolamide Surfactant Nanocarriers for Enhanced Oil Recovery Processes. *Polymers* **2019**, *11* (9), 1513.
(278) Chen, C.; Wang, S.; Kadhum, M. J.; Harwell, J. H.; Shiau, B.-J. Using Carbonaceous Nanoparticles as Surfactant Carrier in Enhanced Oil Recovery: A Laboratory Study. *Fuel* **2018**, *222*, 561–568.
(279) Nourafkan, E.; Hu, Z.; Wen, D. Nanoparticle-Enabled Delivery of Surfactants in Porous Media. *J. Colloid Interface Sci.* **2018**, *519*, 44–57.
(280) Rosestolato, J. C.; Pérez-Gramatges, A.; Lachter, E. R.; Nascimento, R. S. Lipid Nanostructures as Surfactant Carriers for Enhanced Oil Recovery. *Fuel* **2019**, *239*, 403–412.
(281) Romero-Zerón, L. B.; Kittisrisawai, S. Evaluation of a Surfactant Carrier for the Effective Propagation and Target Release of Surfactants within Porous Media during Enhanced Oil Recovery. Part I: Dynamic Adsorption Study. *Fuel* **2015**, *148*, 238–245.
(282) Cortés, F. B.; Lozano, M.; Santamaria, O.; Betancur Marquez, S.; Zapata, K.; Ospina, N.; Franco, C. A. Development and Evaluation of Surfactant Nanocapsules for Chemical Enhanced Oil Recovery (EOR) Applications. *Molecules* **2018**, *23* (7), 1523.
(283) Nourafkan, E.; Hu, Z.; Wen, D. Controlled Delivery and Release of Surfactant for Enhanced Oil Recovery by Nanodroplets. *Fuel* **2018**, *218*, 396–405.
(284) Jang, S. H.; Liyanage, P. J.; Tagavifar, M.; Chang, L.; Upamali, K. A.; Lansakara-P, D.; Weerasooriya, U.; Pope, G. A. A Systematic Method for Reducing Surfactant Retention to Extremely Low Levels. In *SPE Improved Oil Recovery Conference*; Society of Petroleum Engineers, 2016.
(285) Upamali, K. A.; Liyanage, P. J.; Jang, S. H.; Shook, E.; Weerasooriya, U. P.; Pope, G. A. New Surfactants and Cosolvents Increase Oil Recovery and Reduce Cost. *SPE J.* **2018**, *23* (06), 2,202-2,217.
(286) Dwarakanath, V.; Chaturvedi, T.; Jackson, A.; Malik, T.; Siregar, A. A.; Zhao, P. Using Co-Solvents to Provide Gradients and Improve Oil Recovery during Chemical Flooding in a Light

Oil Reservoir. In *SPE Symposium on Improved Oil Recovery*; Society of Petroleum Engineers, 2008.
(287) Arachchilage, G. W.; Alexis, D.; Kim, D. H.; Davidson, A.; Malik, T.; Dwarakanath, V. Systematically Optimized Surfactant Formulation and Injection Design to Reduce Chemical While Maintaining Performance. In *SPE Improved Oil Recovery Conference*; Society of Petroleum Engineers, 2018.
(288) Sahni, V.; Dean, R. M.; Britton, C.; Kim, D. H.; Weerasooriya, U.; Pope, G. A. The Role of Co-Solvents and Co-Surfactants in Making Chemical Floods Robust. In *SPE improved oil recovery symposium*; Society of Petroleum Engineers, 2010.
(289) Jia, H.; Huang, P.; Wang, Q.; Han, Y.; Wang, S.; Dai, J.; Song, J.; Zhang, F.; Yan, H.; Lv, K. Study of a Gemini Surface Active Ionic Liquid 1, 2-Bis (3-Hexylimidazolium-1-Yl) Ethane Bromide as a High Performance Shale Inhibitor and Inhibition Mechanism. *J. Mol. Liq.* **2020**, *301*, 112401.
(290) Nandwani, S.; Malek, N. I.; Chakraborty, M.; Gupta, S. Insight into the Application of Surface-Active Ionic Liquids in Surfactant Based Enhanced Oil Recovery Processes–a Guide Leading to Research Advances. *Energy Fuels* **2020**.
(291) Hanamertani, A. S.; Pilus, R. M.; Idris, A. K.; Irawan, S.; Tan, I. M. Ionic Liquids as a Potential Additive for Reducing Surfactant Adsorption onto Crushed Berea Sandstone. *J. Pet. Sci. Eng.* **2018**, *162*, 480–490.
(292) Hirasaki, G. J.; Van Domselaar, H. R.; Nelson, R. C. Evaluation of the Salinity Gradient Concept in Surfactant Flooding. *Soc. Pet. Eng. J.* **1983**, *23* (03), 486–500.
(293) Tay, A.; Oukhemanou, F.; Wartenberg, N.; Moreau, P.; Guillon, V.; Delbos, A.; Tabary, R. Adsorption Inhibitors: A New Route to Mitigate Adsorption in Chemical Enhanced Oil Recovery. In *SPE Asia Pacific enhanced oil recovery conference*; Society of Petroleum Engineers, 2015.
(294) Nelson, R. C. The Salinity-Requirement Diagram-A Useful Tool in Chemical Flooding Research and Development. *Soc. Pet. Eng. J.* **1982**, *22* (02), 259–270.
(295) Bazin, B.; Tabary, R.; Douarche, F.; Moreau, P.; Oukhemanou, F. Impact of Difficult Environments on Chemical Flooding Performance. In *IOR 2013-17th European Symposium on Improved Oil Recovery*; European Association of Geoscientists & Engineers, 2013; p cp-342-00046.
(296) Al-Murayri, M. T.; Hassan, A. A.; Abdullah, M. B.; Abdulrahim, A. M.; Marliere, C.; Hocine, S.; Tabary, R. Surfactant-Polymer Flooding: Chemical Formulation Design and Evaluation for the Raudhatain Lower Burgan RALB Reservoir in Kuwait. In *SPE Middle East Oil & Gas Show and Conference*; Society of Petroleum Engineers, 2017.
(297) Dang, C.; Nghiem, L.; Nguyen, N.; Chen, Z.; Yang, C.; Bae, W. A Comprehensive Evaluation of Alkaline Surfactant Polymer Flooding and Hybrid Process for Enhanced Oil Recovery. In *SPE annual technical conference and exhibition*; Society of Petroleum Engineers, 2017.
(298) Delamaide, E.; Moreau, P.; Tabary, R. A New Approach for Offshore Chemical Enhanced Oil Recovery. In *Offshore technology conference*; Offshore Technology Conference, 2015.
(299) Tabary, R.; Douarche, F.; Bazin, B.; Lemouzy, P. M.; Moreau, P.; Morvan, M. Design of a Surfactant/Polymer Process in a Hard Brine Context: A Case Study Applied to Bramberge Reservoir. In *SPE EOR conference at oil and gas West Asia*; Society of Petroleum Engineers, 2012.
(300) Morrow, N.; Buckley, J. Improved Oil Recovery by Low-Salinity Waterflooding. *J. Pet. Technol.* **2011**, *63* (05), 106–112.
(301) Sanyal, S.; Bhui, U. K.; Kumar, S. S.; Balaga, D. Designing Injection Water for Enhancing Oil Recovery from Kaolinite Laden Hydrocarbon Reservoirs: A Spectroscopic Approach for Understanding Molecular Level Interaction during Saline Water Flooding. *Energy Fuels* **2017**, *31* (11), 11627–11639.
(302) Sanyal, S.; Bhui, U. K.; Balaga, D.; Kumar, S. S. Interaction Study of Montmorillonite-Crude Oil-Brine: Molecular-Level Implications on Enhanced Oil Recovery during Low Saline Water Flooding from Hydrocarbon Reservoirs. *Fuel* **2019**, *254*, 115725.

(303) Sanyal, S.; Singh, K. A.; Parekh, H.; Chokshi, V.; Bhui, U. K. Interaction Study of Clay-Bearing Amphibolite–Crude Oil–Saline Water: Molecular Level Implications for Enhanced Oil Recovery during Low Saline Water Flooding. *J. Earth Syst. Sci.* **2018**, *127* (8), 1–11.
(304) Shah, D.; Vyas, D.; Bhui, U. K. Interaction of Clay–Crude Oil–Injection Brine: An Experimental Approach for Understanding the Effectiveness of Low Saline Water (LSW) During Enhanced Oil Recovery (EOR). *Macromol. Charact. Hydrocarb. Sustain. Future Appl. Hydrocarb. Value Chain* 43.
(305) Fattahi Mehraban, M.; Farzaneh, S. A.; Sohrabi, M.; Sisson, A. Novel Insights into the Pore-Scale Mechanism of Low Salinity Water Injection and the Improvements on Oil Recovery. *Energy Fuels* **2020**, *34* (10), 12050–12064.
(306) Mehraban, M. F.; Farzaneh, S. A.; Sohrabi, M. Debunking the Impact of Salinity on Crude Oil/Water Interfacial Tension. *Energy Fuels* **2021**, *35* (5), 3766–3779.
(307) Nourani, M.; Tichelkamp, T.; Gaweł, B.; Øye, G. Method for Determining the Amount of Crude Oil Desorbed from Silica and Aluminosilica Surfaces upon Exposure to Combined Low-Salinity Water and Surfactant Solutions. *Energy Fuels* **2014**, *28* (3), 1884–1889.
(308) Farooq, U.; Asif, N.; Tweheyo, M. T.; Sjöblom, J.; Øye, G. Effect of Low-Saline Aqueous Solutions and PH on the Desorption of Crude Oil Fractions from Silica Surfaces. *Energy Fuels* **2011**, *25* (5), 2058–2064.
(309) Liu, X.; Yan, W.; Stenby, E. H.; Thormann, E. Release of Crude Oil from Silica and Calcium Carbonate Surfaces: On the Alternation of Surface and Molecular Forces by High-and Low-Salinity Aqueous Salt Solutions. *Energy Fuels* **2016**, *30* (5), 3986–3993.
(310) Hosseinzade Khanamiri, H.; Nourani, M.; Tichelkamp, T.; Stensen, J. Å.; Øye, G.; Torsæter, O. Low-Salinity-Surfactant Enhanced Oil Recovery (EOR) with a New Surfactant Blend: Effect of Calcium Cations. *Energy Fuels* **2016**, *30* (2), 984–991.
(311) Hosseinzade Khanamiri, H.; Baltzersen Enge, I.; Nourani, M.; Stensen, J. Å.; Torsæter, O.; Hadia, N. EOR by Low Salinity Water and Surfactant at Low Concentration: Impact of Injection and in Situ Brine Composition. *Energy Fuels* **2016**, *30* (4), 2705–2713.
(312) Alagic, E.; Skauge, A. Combined Low Salinity Brine Injection and Surfactant Flooding in Mixed− Wet Sandstone Cores. *Energy Fuels* **2010**, *24* (6), 3551–3559.
(313) Jha, N. K.; Iglauer, S.; Barifcani, A.; Sarmadivaleh, M.; Sangwai, J. S. Low-Salinity Surfactant Nanofluid Formulations for Wettability Alteration of Sandstone: Role of the SiO2 Nanoparticle Concentration and Divalent Cation/SO42–Ratio. *Energy Fuels* **2019**, *33* (2), 739–746.
(314) Youyi, Z.; Zhang, Y.; Jialing, N.; Weidong, L. I. U.; Qingfeng, H. O. U. The Research Progress in the Alkali-Free Surfactant-Polymer Combination Flooding Technique. *Pet. Explor. Dev.* **2012**, *39* (3), 371–376.
(315) Liu, Z.; Bode, V.; Hadayati, P.; Onay, H.; Sudhölter, E. J. Understanding the Stability Mechanism of Silica Nanoparticles: The Effect of Cations and EOR Chemicals. *Fuel* **2020**, *280*, 118650.
(316) Abalkhail, N.; Liyanage, P. J.; Upamali, K. A.; Pope, G. A.; Mohanty, K. K. Alkaline-Surfactant-Polymer Formulation Development for a HTHS Carbonate Reservoir. *J. Pet. Sci. Eng.* **2020**, 107236.
(317) Ghosh, P.; Sharma, H.; Mohanty, K. K. Development of Surfactant-Polymer SP Processes for High Temperature and High Salinity Carbonate Reservoirs. In *SPE Annual Technical Conference and Exhibition*; Society of Petroleum Engineers, 2018.
(318) Ghosh, P.; Mohanty, K. K. Study of Surfactant–Polymer Flooding in High-Temperature and High-Salinity Carbonate Rocks. *Energy Fuels* **2019**, *33* (5), 4130–4145.
(319) Kamal, M. S.; Sultan, A.; Hussein, I.; Hussain, S. M.; AlSofi, A. M. Screening of Surfactants and Polymers for High Temperature High Salinity Carbonate Reservoirs. In *SPE Kingdom of Saudi Arabia Annual Technical Symposium and Exhibition*; Society of Petroleum Engineers, 2018.
(320) Kumar, S.; Saxena, N.; Mandal, A. Synthesis and Evaluation of Physicochemical Properties of Anionic Polymeric Surfactant Derived from Jatropha Oil for Application in Enhanced Oil Recovery. *J. Ind. Eng. Chem.* **2016**, *43*, 106–116.

(321) Elraies, K. A.; Tan, I. M.; Fathaddin, M. T.; Abo-Jabal, A. Development of a New Polymeric Surfactant for Chemical Enhanced Oil Recovery. *Pet. Sci. Technol.* **2011**, *29* (14), 1521–1528.
(322) Johansson, I.; Svensson, M. Surfactants Based on Fatty Acids and Other Natural Hydrophobes. *Curr. Opin. Colloid Interface Sci.* **2001**, *6* (2), 178–188.
(323) Zhang, Q.-Q.; Cai, B.-X.; Xu, W.-J.; Gang, H.-Z.; Liu, J.-F.; Yang, S.-Z.; Mu, B.-Z. Novel Zwitterionic Surfactant Derived from Castor Oil and Its Performance Evaluation for Oil Recovery. *Colloids Surf. Physicochem. Eng. Asp.* **2015**, *483*, 87–95.